

Journal of Mechanics of Materials and Structures

**NONLOCAL FORCED VIBRATION OF A
DOUBLE SINGLE-WALLED CARBON NANOTUBE SYSTEM
UNDER THE INFLUENCE OF AN AXIAL MAGNETIC FIELD**

Marija B. Stamenković, Danilo Karličić, Goran Janevski and Predrag Kozić

Volume 11, No. 3

May 2016



NONLOCAL FORCED VIBRATION OF A DOUBLE SINGLE-WALLED CARBON NANOTUBE SYSTEM UNDER THE INFLUENCE OF AN AXIAL MAGNETIC FIELD

MARIJA B. STAMENKOVIĆ, DANILO KARLIČIĆ, GORAN JANEVSKI AND PREDRAG KOZIĆ

The influence of various physical phenomena on the dynamic behavior of nanostructures has been attracting more and more attention of the scientific community. This paper discusses the effects of the axial magnetic field on the externally excited double single-walled carbon nanotube (DSWCNT) coupled by a Winkler elastic medium. It is assumed that both carbon nanotubes are identical and under the influence of compressive axial load with simply supported ends. Based on the Eringen nonlocal elasticity and Euler–Bernoulli beam theory, the system of two coupled nonhomogeneous partial differential equations of motion is derived, where the effects of the Lorentz magnetic force are obtained via a Maxwell relation. The dynamic responses of the DSWCNT system for four different cases of external transversal load are considered. The closed form solutions for the transversal displacements are obtained by applying the Bernoulli–Fourier method of particular integrals on the system of nonhomogeneous partial differential equations of motion. Also, analytical expressions of the amplitude ratio for forced vibration are derived and then validated with existing results. Moreover, the obtained analytical results for fundamental natural frequency are validated with results obtained by molecular dynamics (MD) simulation and show fine agreements. The effects of compressive axial load, nonlocal parameter, axial magnetic field and stiffness coefficient of the elastic medium on the forced dynamic behavior of DSWCNT are considered through numerical examples. From numerical results we can conclude that the dynamical behavior of DSWCNT is greatly influenced by the magnetic field and nonlocal parameter. Furthermore, by selecting the intensity of the axial magnetic field in a certain range, it is possible to adjust the stiffness of the system without changing the material and geometric parameters. This effect implies a change in the natural frequencies of the system.

1. Introduction

In the last few decades, carbon nanotubes (CNTs) [Iijima 1991; Hata et al. 2004; Iijima et al. 1996] have drawn considerable attention from scientists and engineers in the field of nanotechnology due to their extraordinary physical [Reich et al. 2008], chemical [Hu et al. 1999], and mechanical properties [Lu 1997]. Salvetat et al. [1999] explain the properties of nanotubes in the wider context of materials science, where experimental results confirm the theoretical predictions that carbon nanotubes have high strength, extraordinary flexibility and resilience. Moreover, these superior characteristics provide them with a wide range of applications in nanoscale devices, such as biosensors [Murmu and Adhikari 2012; Adhikari and Chowdhury 2010], mass sensors [Murmu and Adhikari 2011; Li and Chou 2004], nanoactuators [Li et al. 2008; Roth and Baughman 2002], field emitters [Saito 2003], nanoelectronic

Keywords: forced vibration, nonlocal elasticity, axial magnetic field, analytical solution, carbon nanotubes.

devices [Avouris et al. 2007], and fillers for nanocomposite structures [Moniruzzaman and Winey 2006; Ajayan et al. 2006]. Single-walled carbon nanotubes (SWCNT) are cylindrical macromolecules obtained in specific technological processes by rolling the two-dimensional structures such as graphene sheets into a tube. Based on the experimental analyses [Ruoff et al. 2003; Dresselhaus et al. 2005] and atomistic theories [Dubay and Kresse 2003; Liu et al. 2003], it has been shown that the “size-effect” plays an important role in describing the physical and mechanical properties of materials on the nanoscale level of CNTs. However, conducting experiments on the nano level is a very complex and expensive task due to difficulties in the control of all system parameters.

Furthermore, an atomistic theory such as molecular dynamic (MD) simulation [Duan et al. 2007] is suitable only for systems with a small number of particles; such theories can be expensive in view of time or computational resources for larger systems. Due to the disadvantages of these two methods, researchers are increasingly turning to models obtained through continuum mechanics. However, because of the existence of small-scale effects, the classical continuum theories need to be reformulated to take these effects into account.

This can be done by introducing nonlocality in the space domain, modifying the corresponding constitutive equation and introducing the material parameter, which takes into account the effects of length scale and influence of the interatomic forces. One of the first scale-dependent continuum theories proposed by Eringen and coworkers [Eringen 1972; 1983; Eringen and Edelen 1972], which takes nonlocal effects into account is known as the nonlocal elasticity theory. According to Eringen [2002], the nonlocal theory gives great approximation for a large class of problems in nanosystems where the influence of length-scales is very pronounced. Yang et al. [2010] investigated nonlinear free vibration of single-walled carbon nanotubes (SWCNTs), while Ke et al. [2009] investigated nonlinear free vibration of embedded double-walled carbon nanotubes (DWCNTs), based on Eringen’s nonlocal elasticity theory and von Kármán geometric nonlinearity.

Consideration of magnetic field effects is important to complete the knowledge of the mechanical behavior of nanomaterials such as CNTs [Bellucci et al. 2007; Correa-Duarte et al. 2005] and graphene sheets [Goerbig et al. 2006; Ghorbanpour Arani and Shokravi 2014]. Arani et al. [2013] studied thermally nonlocal vibration of a double bounded graphene sheet under the influence of two-dimensional magnetic field with biaxial in-plane load. They obtained a numerical solution of the coupled partial differential equation by the differential quadrature method for simply supported boundary conditions and analyzed the influences of the magnetic field on the frequency ratio. Based on the nonlocal elasticity theory, Kiani [2012] reformulated Rayleigh, Timoshenko and higher-order beam theories for modeling wave propagation in embedded SWCNT under the influence of an axial magnetic field. The authors derived phase and group velocity and investigated the influence of small-scale parameters, longitudinal magnetic field stiffness coefficients of the surrounding medium on the flexural and shear waves. Narendar et al. [2012] analyzed the effects of a longitudinal magnetic field on wave dispersion characteristics of SWCNT embedded in a Pasternak elastic medium in the framework of nonlocal elasticity. They found that the nonlocality reduces the wave velocity in the presence of a magnetic field, but without the influence on the higher frequency region. In the paper proposed by Murmu et al. [2012b], authors considered transversal vibration of magnetic influenced double walled carbon nanotubes (DWCNT) according to the Eringen nonlocal continuum theory. Analytical solutions of natural frequency and transversal displacements of DWCNT were obtained for simply supported boundary conditions. Also, the effects of different materials

parameters on the vibration behavior were analyzed and discussed in detail. Consideration of the effects of an axial magnetic field on the dynamical behavior of double single-walled carbon nanotubes using the nonlocal Euler–Bernoulli beam theory is shown in the work of Murmu et al. [2012a]. Applying a method of separation of variables, they solved the system of two coupled partial differential equations and obtained a closed form solution for natural frequency. The effects of a nonlocal parameter and intensity of longitudinal magnetic field on the synchronous and asynchronous vibration phases of a double single walled carbon system were also investigated. Karličić et al. [2014c] investigated the influence of damping and axial magnetic field effects on the vibration behavior of a viscoelasticity system of m coupled carbon nanotubes based on the nonlocal viscoelasticity theory. They obtained an analytical solution for damping natural frequency, damping ratio and their critical values in the case when the mode and number of nanotubes tend to infinity.

The modeling of forced vibration states in nanosystems becomes a more and more important part in the design of MEMS and NEMS devices [Kacem et al. 2011; Lazarus et al. 2012]. Based on the Kirchhoff plate theory and Eringen constitutive relation, governing equations of motion are derived and then solved by using the Galerkin procedures for vibration frequencies and forced response. Aksencer and Aydogdu [2012] investigated forced vibration of nanoplates by using the nonlocal elasticity and Kirchhoff plate theory. The Navier-type solution method was used for simply supported nanoplates where forced vibration response was obtained in the analytical form. Claeysen et al. [2013] explored the forced response of a single carbon nanotube modeled via the nonlocal Euler–Bernoulli beam theory. Forced responses were determined for different external loads and boundary conditions using the Galerkin method. Recently, researchers have focused their investigations on the particular problem of forced vibration such as the influence of moving nanoparticles on nanostructural elements such as nanotubes and nanoplates [Kiani and Mehri 2010; Şimşek 2010a]. Şimşek [2011] presented an analytical method for the forced vibration of an elastically connected double-carbon nanotube system carrying a moving nanoparticle based on the nonlocal elasticity and Euler–Bernoulli beam theory. The closed-form solutions for the dynamic deflections of the two nanobeams were derived for two sets of critical velocity, and then effects of the nonlocal parameter, aspect ratio, velocity of the moving nanoparticle and the elastic layer between the nanotubes on the dynamic responses were discussed. Zhang et al. [2008] introduced compressive axial load on the external excited double beam system. They obtained analytical solutions of forced vibration responses for two cases of particular excitation loadings. Oniszczuk [2003] analyzed undamped forced transverse vibrations of an elastically connected complex double-beam system, based on the Euler–Bernoulli beam and classical elasticity theory. Several cases of particularly interesting excitation loadings such as of stationary harmonic loads and moving forces were investigated.

In this paper, using the Euler–Bernoulli beam theory we analyze the effects of axial compressive load and magnetic field on the forced transversal vibration of a magnetically sensitive double SWCNT system. The Eringen nonlocal continuum theory is used to introduce small-scale effects via a material parameter. It is assumed that the double coupled SWCNT system is modeled as a system of two slender parallel nanobeams elastically connected by a Winkler elastic medium. The system of two coupled partial differential equations of motion is derived by considering the nonlocal Euler–Bernoulli beam theory and classical Maxwell relation. Analytical solutions for natural frequencies, amplitude ratio and forced response in four cases of external excitation load are determined by applying the Bernoulli–Fourier methods. Numerical simulations show that the nonlocal parameter and intensity of axial magnetic fields

have a significant influence on the natural frequencies and dynamical response of the DSWCNT system. It should be noted that this study is limited only to the armchair SWCNT system, where the influence of rotation of magnetically influenced nanotubes is neglected [Popov et al. 2014; Krstić et al. 2004; Slavcheva and Roussignol 2011]. Then molecular dynamics (MD) simulation is implemented to obtain fundamental frequencies of nanotubes for armchair SWCNT and values of aspect ratio to compare them with the results obtained by the nonlocal beam models, presented by Ansari and Sahmani [2012] and Ansari et al. [2012]. The results presented here are validated with the results found in the literature.

2. Problem formulation

2.1. Nonlocal elastic constitutive relation. The fundamental equations of the nonlocal elasticity theory are considered in this section. The basic assumption in this continuum theory is that the stress at a point is a function of the strains at all points of the whole body. The constitutive elastic relation for a three-dimensional homogeneous isotropic body in the integral form is given by Eringen and coworkers [Eringen 1972; Eringen and Edelen 1972] as

$$\sigma_{ij}(x) = \int \alpha(|x - x'|, \tau) C_{ijkl} \epsilon_{kl}(x') dV(x') \quad \text{for all } x \in V, \quad (1a)$$

$$\sigma_{ij,j} = 0, \quad (1b)$$

$$\epsilon_{ij} = \frac{1}{2}(u_{i,j} + u_{j,i}), \quad (1c)$$

where C_{ijkl} is the elastic modulus tensor for classical isotropic elasticity; σ_{ij} and ϵ_{ij} are the stress and the strain tensors, respectively, and u_i is the displacement vector. By $\alpha(|x - x'|, \tau)$ we denote the nonlocal modulus or attenuation function, which incorporates nonlocal effects into the constitutive equation at a reference point x produced by the local strain at a source x' . The above absolute value of the difference $|x - x'|$ denotes the Euclidean metric, and τ is the parameter $\tau = (e_0 a)/l$, where l is the external characteristic length (crack length, wave length), a describes the internal characteristic length (lattice parameter, granular size and distance between C-C bounds) and e_0 is a constant appropriate to each material that can be identified from atomistic simulations or by using the dispersive curve of the Born–Karman model of lattice dynamics.

As Equation (1) is difficult to use in practical examples, simplified constitutive relations in the differential form are developed. According to Eringen [1983], constitutive relations in differential form are given as

$$\sigma_{xx} - \mu \frac{d^2 \sigma_{xx}}{dx^2} = E \epsilon_{xx}, \quad (2)$$

$$\sigma_{xz} - \mu \frac{d^2 \sigma_{xz}}{dx^2} = G \gamma_{xz}, \quad (3)$$

where E and G are the elastic modulus and the shear modulus of the beam, respectively, $\mu = (e_0 a)^2$ is the nonlocal parameter, σ_{xx} , σ_{xz} are the normal and the shear nonlocal stresses, respectively, and $\epsilon_{xx} = \partial u / \partial x$ is the axial deformation. The internal characteristic lengths ($e_0 a$) are often assumed to be in the range 0–2 [nm] for nanomaterials such as carbon nanotubes, zinc oxide, etc. When $e_0 a = 0$, the nonlocal constitutive relation is reduced to the classical constitutive relation of the elastic body.

2.2. Maxwell's relation. According to Murmu et al. [2012b; 2012a], the equation which connects the current density \mathbf{J} , distributing vector of magnetic field \mathbf{h} , strength vector of the electric fields \mathbf{e} , and magnetic field permeability η , is represented by Maxwell's expressions [Kraus 1984] as

$$\mathbf{J} = \nabla \times \mathbf{h}, \quad \nabla \times \mathbf{e} = -\eta \frac{\partial \mathbf{h}}{\partial t}, \quad \nabla \cdot \mathbf{h} = 0, \quad (4)$$

where the vectors of distributing magnetic field \mathbf{h} and the electric field \mathbf{e} are defined as

$$\mathbf{h} = \nabla \times (\mathbf{U} \times \mathbf{H}), \quad \mathbf{e} = -\eta \left(\frac{\partial \mathbf{U}}{\partial t} \times \mathbf{H} \right), \quad (5)$$

in which $\nabla = (\partial/\partial x)\mathbf{i} + (\partial/\partial y)\mathbf{j} + (\partial/\partial z)\mathbf{k}$ is the Hamilton operator, $\mathbf{U} = (x, y, z)$ is the displacement vector and $\mathbf{H} = (H_x, 0, 0)$ is the vector of the axial magnetic field. In the present study, we assume that the axial magnetic field acts on the double SWCNT in the x -direction of the system. Now, we can write the vector of the distributing magnetic field [Murmu et al. 2012b; 2012a] in the form

$$\mathbf{h} = -H_x \left(\frac{\partial v}{\partial y} + \frac{\partial w}{\partial z} \right) \mathbf{i} + H_x \frac{\partial v}{\partial x} \mathbf{j} + H_x \frac{\partial w}{\partial x} \mathbf{k}. \quad (6)$$

Then we introduce (6) into the first expression of (4):

$$\mathbf{J} = \nabla \times \mathbf{h} = H_x \left(-\frac{\partial^2 v}{\partial x \partial z} + \frac{\partial^2 w}{\partial x \partial y} \right) \mathbf{i} - H_x \left(\frac{\partial^2 v}{\partial y \partial z} + \frac{\partial^2 w}{\partial x^2} + \frac{\partial^2 w}{\partial z^2} \right) \mathbf{j} + H_x \left(\frac{\partial^2 v}{\partial x^2} + \frac{\partial^2 v}{\partial y^2} + \frac{\partial^2 w}{\partial z \partial y} \right) \mathbf{k}. \quad (7)$$

Introducing (7) into the expressions for the Lorentz force induced by the axial magnetic field yields

$$\mathbf{f} = f_x \mathbf{i} + f_y \mathbf{j} + f_z \mathbf{k} = \eta (\mathbf{J} \times \mathbf{H}), \quad (8)$$

where f_x , f_y and f_z express the Lorentz force along the x , y and z directions, as follows:

$$f_x = 0, \quad (9a)$$

$$f_y = \eta H_x^2 \left(\frac{\partial^2 v}{\partial x^2} + \frac{\partial^2 v}{\partial y^2} + \frac{\partial^2 w}{\partial z \partial y} \right), \quad (9b)$$

$$f_z = \eta H_x^2 \left(\frac{\partial^2 w}{\partial x^2} + \frac{\partial^2 w}{\partial y^2} + \frac{\partial^2 v}{\partial z \partial y} \right). \quad (9c)$$

We assume that the transversal displacements of the first and second SWCNT in the system are denoted as $w_1(x, t)$ and $w_2(x, t)$, respectively, and the Lorentz force acts only in the z direction, which can be written as

$$f_{z,i} = \eta H_x^2 \frac{\partial^2 w_i}{\partial x^2}, \quad i = 1, 2. \quad (10)$$

Finally, it is possible to obtain force per unit length of both SWCNTs in the system as

$$\tilde{q}_i(x, t) = \int_A f_{z,i} dA = \eta A H_x^2 \frac{\partial^2 w_i}{\partial x^2}, \quad i = 1, 2. \quad (11)$$

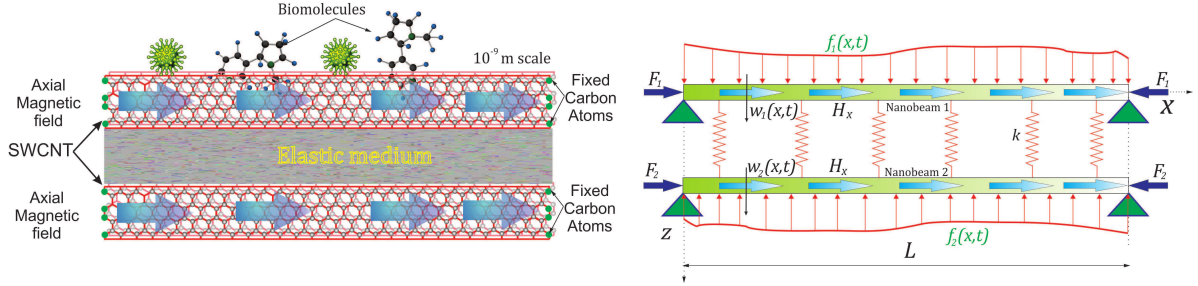


Figure 1. The system of double SWCNT affected by an axial magnetic field. Left: the physical model of external excited DSWCNTs with fixed single layer of carbon atoms [Ansari and Sahmani 2012] coupled by an elastic medium and influenced by an axial magnetic field. Right: the equivalent mechanical model.

2.3. Mathematical model. Consider a compressive nonlocal double SWCNT system which is under the influence of an axial magnetic field as shown in Figure 1, left. The nonlocal double SWCNT system is assumed to be modeled as a system composed of two parallel nanobeams, which have the same length and are continuously joined by a Winkler elastic layer. It should be noted that the fixed atomic layers on the sides of the carbon nanotubes represent, from the mechanical point of view, simply supported boundary conditions, as shown in [Ansari and Sahmani 2012]. The stiffness modulus of the Winkler elastic layer is denoted with k . The transversal displacement over the two nanobeams is denoted by $w_1(x, t)$ and $w_2(x, t)$, respectively; see Figure 1, right. For the sake of simplicity, we will consider only the case of identical nanobeams, where geometric and physical properties are the same for both nanobeams and defined as follows: A is the cross-sectional area, E is the Young's modulus, ρ is the mass density, I is the moment of inertia and L is the length of the nanobeam. Also, we assume that nanobeams 1 and 2 are subjected to positive axial compressions F_1 and F_2 and arbitrarily distributed transverse continuous loads $f_1(x, t)$ and $f_2(x, t)$, respectively, that are positive when they act downward. The influence of the Lorentz magnetic force on the double nanobeam system is caused by the axial magnetic field which acts in the x direction, as shown in Figure 1.

Using the Euler–Bernoulli beam theory and Eringen nonlocal elasticity following the methodology presented in the work of Kozic et al. [2014], the governing equations of motion of the nonlocal double nanobeam system (NDNBS) can be given as

$$\begin{aligned} \rho A \frac{\partial^2 w_1}{\partial t^2} - f_1 + k(w_1 - w_2) + F_1 \frac{\partial^2 w_1}{\partial x^2} - \eta A H_x^2 \frac{\partial^2 w_1}{\partial x^2} + EI \frac{\partial^4 w_1}{\partial x^4} \\ = \mu \frac{\partial^2}{\partial x^2} \left[\rho A \frac{\partial^2 w_1}{\partial t^2} - f_1 + k(w_1 - w_2) + F_1 \frac{\partial^2 w_1}{\partial x^2} - \eta A H_x^2 \frac{\partial^2 w_1}{\partial x^2} \right], \end{aligned} \quad (12)$$

$$\begin{aligned} \rho A \frac{\partial^2 w_2}{\partial t^2} - f_2 - k(w_1 - w_2) + F_2 \frac{\partial^2 w_2}{\partial x^2} - \eta A H_x^2 \frac{\partial^2 w_2}{\partial x^2} + EI \frac{\partial^4 w_2}{\partial x^4} \\ = \mu \frac{\partial^2}{\partial x^2} \left[\rho A \frac{\partial^2 w_2}{\partial t^2} - f_2 - k(w_1 - w_2) + F_2 \frac{\partial^2 w_2}{\partial x^2} - \eta A H_x^2 \frac{\partial^2 w_2}{\partial x^2} \right]. \end{aligned} \quad (13)$$

The boundary conditions of the NDNBS are assumed to be simply supported and considered as

$$w_i(0, t) = w_i(L, t) = 0, \quad (14)$$

$$\frac{\partial^2 w_i}{\partial x^2}(0, t) = \frac{\partial^2 w_i}{\partial x^2}(L, t) = 0, \quad i = 1, 2, \quad (15)$$

where L is the length of the two nanobeams, and t is the time.

In order to simplify the solving of Equations (12) and (13), we introduce the dimensionless parameters

$$\begin{aligned} \mu = L^2 \eta^2, \quad x = L\xi, \quad L = \frac{x}{\xi}, \quad t^2 = \tau^2 L^4 c^2, \quad c^2 = \frac{\rho A}{EI}, \quad \bar{f}_i = \frac{L^3}{EI} f_i, \\ \bar{F}_i = \frac{L^2 F_i}{EI}, \quad K = \frac{kL^4}{EI}, \quad \text{MP} = \frac{L^2}{EI} \eta A H_x^2, \quad w_i = L \bar{w}_i, \quad i = 1, 2. \end{aligned} \quad (16)$$

Introducing dimensionless parameters (16) into Equations (12) and (13), we can write the system of partial differential equations as

$$\begin{aligned} \frac{\partial^2 \bar{w}_1}{\partial \tau^2} + K(\bar{w}_1 - \bar{w}_2) + (\bar{F}_1 - \text{MP}) \frac{\partial^2 \bar{w}_1}{\partial \xi^2} + \frac{\partial^4 \bar{w}_1}{\partial \xi^4} \\ - \eta^2 \frac{\partial^2}{\partial \xi^2} \left[\frac{\partial^2 \bar{w}_1}{\partial \tau^2} + K(\bar{w}_1 - \bar{w}_2) + (\bar{F}_1 - \text{MP}) \frac{\partial^2 \bar{w}_1}{\partial \xi^2} \right] = \bar{f}_1 - \eta^2 \frac{\partial^2 \bar{f}_1}{\partial \xi^2}, \end{aligned} \quad (17)$$

$$\begin{aligned} \frac{\partial^2 \bar{w}_2}{\partial \tau^2} - K(\bar{w}_1 - \bar{w}_2) + (\bar{F}_2 - \text{MP}) \frac{\partial^2 \bar{w}_1}{\partial \xi^2} + \frac{\partial^4 \bar{w}_1}{\partial \xi^4} \\ - \eta^2 \frac{\partial^2}{\partial \xi^2} \left[\frac{\partial^2 \bar{w}_1}{\partial \tau^2} - K(\bar{w}_1 - \bar{w}_2) + (\bar{F}_2 - \text{MP}) \frac{\partial^2 \bar{w}_1}{\partial \xi^2} \right] = \bar{f}_2 - \eta^2 \frac{\partial^2 \bar{f}_2}{\partial \xi^2}, \end{aligned} \quad (18)$$

where ξ is the dimensionless axial coordinate, and τ is the dimensionless time. Expressions (17) and (18) represent dimensionless governing equations of motion of the NDNBS shown in Figure 1, right.

3. Analytical solution of equations

3.1. Free vibrations. The homogeneous governing partial differential equations (17) and (18) of the NDNBS with boundary conditions (14) and (15) can be solved by the Bernoulli–Fourier method, assuming the solutions in the forms

$$\bar{w}_1(\xi, \tau) = \sum_{n=1}^{\infty} X_n(\xi) T_{1n}(\tau), \quad (19)$$

$$\bar{w}_2(\xi, \tau) = \sum_{n=1}^{\infty} X_n(\xi) T_{2n}(\tau), \quad (20)$$

where $T_{1n}(\tau)$ and $T_{2n}(\tau)$ denote the unknown dimensionless time functions, and $X_n(\xi)$ is the known mode shape function for the simply supported single nanobeam, which is defined as

$$X_n(\xi) = \sin(k_n \xi), \quad (21)$$

with

$$k_n = n\pi, \quad n = 1, 2, 3, \dots \quad (22)$$

The substitution of Equations (19) and (20) into Equations (17) and (18), neglecting the external transversal load \bar{f}_1 and \bar{f}_2 , yields

$$\ddot{T}_{1n} + \left[K - (\bar{F}_1 - MP)k_n^2 + \frac{k_n^4}{1 + \eta^2 k_n^2} \right] T_{1n} - K T_{2n} = 0, \quad (23)$$

$$\ddot{T}_{2n} + \left[K - (\bar{F}_2 - MP)k_n^2 + \frac{k_n^4}{1 + \eta^2 k_n^2} \right] T_{2n} - K T_{1n} = 0. \quad (24)$$

We assume the solutions of differential equations (23) and (24) in the forms

$$T_{1n} = C_n e^{j\omega_n \tau}, \quad T_{2n} = D_n e^{j\omega_n \tau}, \quad j = \sqrt{-1}, \quad (25)$$

where ω_n denotes the natural frequency of the double-nanobeam system, and C_n and D_n represent the amplitude coefficients of the two nanobeams, respectively. Substituting (25) into (23) and (24) yields

$$\begin{bmatrix} K - (\bar{F}_1 - MP)k_n^2 + \frac{k_n^4}{1 + \eta^2 k_n^2} - \omega_n^2 & -K \\ -K & K - (\bar{F}_2 - MP)k_n^2 + \frac{k_n^4}{1 + \eta^2 k_n^2} - \omega_n^2 \end{bmatrix} \begin{Bmatrix} C_n \\ D_n \end{Bmatrix} = \begin{Bmatrix} 0 \\ 0 \end{Bmatrix}. \quad (26)$$

Nontrivial solutions for the constants C_n and D_n can be obtained only when the determinant of the coefficients in equations (26) vanishes. This gives the following frequency equation:

$$\begin{aligned} \omega_n^4 - \omega_n^2 \left[2K - \bar{F}_1 k_n^2 - \bar{F}_2 k_n^2 + 2MPk_n^2 + 2\frac{k_n^4}{1 + \eta^2 k_n^2} \right] \\ + \left[K - (\bar{F}_1 - MP)k_n^2 + \frac{k_n^4}{1 + \eta^2 k_n^2} \right] \left[K - (\bar{F}_2 - MP)k_n^2 + \frac{k_n^4}{1 + \eta^2 k_n^2} \right] - K^2 = 0. \end{aligned} \quad (27)$$

From (27) we obtain

$$\omega_{nI}^2 = \frac{1}{2} [b - \sqrt{b^2 - 4c}], \quad (28)$$

$$\omega_{nII}^2 = \frac{1}{2} [b + \sqrt{b^2 - 4c}], \quad (29)$$

where ω_{nI} is the lower natural frequency of the system, and ω_{nII} is the higher natural frequency. In the relations (28) and (29) the parameters are given as

$$b = \left[2K - \bar{F}_1 k_n^2 - \bar{F}_2 k_n^2 + 2MPk_n^2 + 2\frac{k_n^4}{1 + \eta^2 k_n^2} \right], \quad (30)$$

$$c = \left[K - (\bar{F}_1 - MP)k_n^2 + \frac{k_n^4}{1 + \eta^2 k_n^2} \right] \left[K - (\bar{F}_2 - MP)k_n^2 + \frac{k_n^4}{1 + \eta^2 k_n^2} \right] - K^2. \quad (31)$$

For each of the natural frequencies, the associated amplitude ratio of vibration modes of the two nanobeams is given by

$$\alpha_{ni} = \frac{D_{ni}}{C_{ni}} = \frac{K - (\bar{F}_1 - \text{MP})k_n^2 + \frac{k_n^4}{1+\eta^2k_n^2} - \omega_{ni}^2}{K} = \frac{K}{K - (\bar{F}_2 - \text{MP})k_n^2 + \frac{k_n^4}{1+\eta^2k_n^2} - \omega_{ni}^2}, \quad i = \text{I, II}. \quad (32)$$

By entering $\omega_{n\text{I}}^2$ and $\omega_{n\text{II}}^2$ from (28) and (29) into (32), respectively, we obtain

$$3\alpha_{n\text{I}} = \frac{K - (\bar{F}_1 - \text{MP})k_n^2 + \frac{k_n^4}{1+\eta^2k_n^2} - \omega_{n\text{I}}^2}{K} = \frac{K}{K - (\bar{F}_2 - \text{MP})k_n^2 + \frac{k_n^4}{1+\eta^2k_n^2} - \omega_{n\text{I}}^2}, \quad (33)$$

$$\alpha_{n\text{II}} = \frac{K - (\bar{F}_1 - \text{MP})k_n^2 + \frac{k_n^4}{1+\eta^2k_n^2} - \omega_{n\text{II}}^2}{K} = \frac{K}{K - (\bar{F}_2 - \text{MP})k_n^2 + \frac{k_n^4}{1+\eta^2k_n^2} - \omega_{n\text{II}}^2}. \quad (34)$$

3.2. Forced vibrations. The above analysis showed the solution of the homogeneous system of partial differential equations. In the following analysis we will consider the nonhomogeneous differential equations (17) and (18) representing forced vibrations of the (SWCNT) system, assuming solutions in the forms

$$\bar{w}_1(\xi, \tau) = \sum_{n=1}^{\infty} X_n(\xi) \sum_{i=\text{I}}^{\text{II}} S_{ni}(\tau), \quad (35)$$

$$\bar{w}_2(\xi, \tau) = \sum_{n=1}^{\infty} X_n(\xi) \sum_{i=\text{I}}^{\text{II}} \alpha_{ni} S_{ni}(\tau), \quad (36)$$

where $S_{ni}(\tau)$, $i = \text{I, II}$, denote the unknown dimensionless time functions corresponding to the natural frequencies ω_{ni} , $i = \text{I, II}$. Introduction (35) and (36) into (17) and (18), we obtain

$$\sum_{n=1}^{\infty} X_n \sum_{i=\text{I}}^{\text{II}} \left[\ddot{S}_{ni} + \left(K - (\bar{F}_1 - \text{MP})k_n^2 + \frac{k_n^4}{1+\eta^2k_n^2} - K\alpha_{ni} \right) S_{ni} \right] (1+\eta^2k_n^2) = \bar{f}_1 - \eta^2 \frac{\partial^2 \bar{f}_1}{\partial \xi^2}, \quad (37)$$

$$\sum_{n=1}^{\infty} X_n \sum_{i=\text{I}}^{\text{II}} \left[\ddot{S}_{ni} + \left(K - (\bar{F}_2 - \text{MP})k_n^2 + \frac{k_n^4}{1+\eta^2k_n^2} - K\alpha_{ni}^{-1} \right) S_{ni} \right] (1+\eta^2k_n^2)\alpha_{ni} = \bar{f}_2 - \eta^2 \frac{\partial^2 \bar{f}_2}{\partial \xi^2}. \quad (38)$$

By multiplying relations (37) and (38) by the mode shape function $X_m(\xi)$, then integrating with respect to ξ from 0 to 1 and using the orthogonality condition

$$\int_0^1 X_m(\xi) X_n(\xi) d\xi = \int_0^1 \sin(m\pi\xi) \sin(n\pi\xi) d\xi = \beta \delta_{mn} = \int_0^1 X_n^2(\xi) d\xi = \frac{1}{2}, \quad (39)$$

where δ_{mn} is the Kronecker delta function, we have

$$\sum_{i=1}^{\text{II}} \left[\ddot{S}_{ni} + \left(K - (\bar{F}_1 - \text{MP})k_n^2 + \frac{k_n^4}{1 + \eta^2 k_n^2} - K\alpha_{ni} \right) S_{ni} \right] = 2M \int_0^1 \left(\bar{f}_1 - \eta^2 \frac{\partial^2 \bar{f}_1}{\partial \xi^2} \right) X_n(\xi) d\xi, \quad (40)$$

$$\sum_{i=1}^{\text{II}} \left[\ddot{S}_{ni} + \left(K - (\bar{F}_2 - \text{MP})k_n^2 + \frac{k_n^4}{1 + \eta^2 k_n^2} - K\alpha_{ni}^{-1} \right) S_{ni} \right] \alpha_{ni} = 2M \int_0^1 \left(\bar{f}_2 - \eta^2 \frac{\partial^2 \bar{f}_2}{\partial \xi^2} \right) X_n(\xi) d\xi, \quad (41)$$

with

$$M = \frac{1}{1 + \eta^2 k_n^2}. \quad (42)$$

By combining equations (33), (34), (40) and (41) we obtain

$$\sum_{i=1}^{\text{II}} [\ddot{S}_{ni} + \omega_{ni}^2 S_{ni}] = 2M \int_0^1 \left(\bar{f}_1 - \eta^2 \frac{\partial^2 \bar{f}_1}{\partial \xi^2} \right) X_n(\xi) d\xi, \quad (43)$$

$$\sum_{i=1}^{\text{II}} [\ddot{S}_{ni} + \omega_{ni}^2 S_{ni}] \alpha_{ni} = 2M \int_0^1 \left(\bar{f}_2 - \eta^2 \frac{\partial^2 \bar{f}_2}{\partial \xi^2} \right) X_n(\xi) d\xi. \quad (44)$$

From equations (43) and (44) we obtain

$$\ddot{S}_{ni} + \omega_{ni}^2 S_{ni} = R_{ni}(\tau), \quad i = \text{I, II}, \quad (45)$$

where

$$R_{n\text{I}} = 2M \frac{1}{\alpha_{n\text{II}} - \alpha_{n\text{I}}} \int_0^1 \left[\alpha_{n\text{II}} \left(\bar{f}_1 - \eta^2 \frac{\partial^2 \bar{f}_1}{\partial \xi^2} \right) - \left(\bar{f}_2 - \eta^2 \frac{\partial^2 \bar{f}_2}{\partial \xi^2} \right) \right] X_n(\xi) d\xi, \quad (46)$$

$$R_{n\text{II}} = 2M \frac{1}{\alpha_{n\text{I}} - \alpha_{n\text{II}}} \int_0^1 \left[\alpha_{n\text{I}} \left(\bar{f}_1 - \eta^2 \frac{\partial^2 \bar{f}_1}{\partial \xi^2} \right) - \left(\bar{f}_2 - \eta^2 \frac{\partial^2 \bar{f}_2}{\partial \xi^2} \right) \right] X_n(\xi) d\xi. \quad (47)$$

From the equations (45) we obtain

$$S_{ni}(\tau) = \frac{1}{\omega_{ni}} \int_0^\tau R_{ni}(s) \sin[\omega_{ni}(\tau - s)] ds, \quad i = \text{I, II}. \quad (48)$$

By combining (35), (36) and (48), the forced vibrations of the (SWCNT) system can be described by

$$\bar{w}_1(\xi, \tau) = \sum_{n=1}^{\infty} \sin(n\pi\xi) \sum_{i=1}^{\text{II}} \frac{1}{\omega_{ni}} \int_0^\tau R_{ni}(s) \sin[\omega_{ni}(\tau - s)] ds, \quad (49)$$

$$\bar{w}_2(\xi, \tau) = \sum_{n=1}^{\infty} \sin(n\pi\xi) \sum_{i=\alpha_{ni}}^{\text{II}} \alpha_{ni} \frac{1}{\omega_{ni}} \int_0^\tau R_{ni}(s) \sin[\omega_{ni}(\tau - s)] ds. \quad (50)$$

Solutions (49) and (50) can be used to find the dynamic responses of this system for an arbitrary exciting transversal loading in cases with both stationary and moving loads. For the sake of simplicity

in further consideration, it is assumed that only the first nanobeam is subjected to the exciting load. Introducing $\bar{f}_1(\xi, \tau) \neq 0$ and $\bar{f}_2(\xi, \tau) = 0$ into (46) and (47), we obtain

$$R_{nI} = 2M \frac{\alpha_{nII}}{\alpha_{nII} - \alpha_{nI}} \int_0^1 \left(\bar{f}_1 - \eta^2 \frac{\partial^2 \bar{f}_1}{\partial \xi^2} \right) \sin(n\pi\xi) d\xi, \quad (51)$$

$$R_{nII} = 2M \frac{\alpha_{nI}}{\alpha_{nI} - \alpha_{nII}} \int_0^1 \left(\bar{f}_1 - \eta^2 \frac{\partial^2 \bar{f}_1}{\partial \xi^2} \right) \sin(n\pi\xi) d\xi. \quad (52)$$

In the following, we conduct an analysis of forced vibrations for four cases of exciting loadings: uniformly distributed harmonic continuous load, concentrated harmonic force, moving constant force F and moving harmonic force.

3.2.1. Uniformly distributed harmonic load. The uniformly distributed harmonic load

$$\bar{f}_1(\xi, \tau) = r \sin(\Omega\tau) \quad (53)$$

acts upon the SWCNT system (see Figure 2), where r is the amplitude and Ω is the frequency of the exciting harmonic load. By substituting Equation (53) into (51) and (52), we obtain

$$R_{nI} = 4Mr \frac{\alpha_{nII}}{n\pi(\alpha_{nII} - \alpha_{nI})} \sin(\Omega s), \quad n = 1, 3, 5, \dots, \quad (54)$$

$$R_{nII} = 4Mr \frac{\alpha_{nI}}{n\pi(\alpha_{nI} - \alpha_{nII})} \sin(\Omega s), \quad n = 1, 3, 5, \dots \quad (55)$$

The introduction of equations (54) and (55) into equations (49) and (50) gives

$$\bar{w}_1(\xi, \tau) = \sum_{n=1}^{\infty} \sin(n\pi\xi) \left[A_{nI} \sin(\Omega\tau) + \sum_{i=1}^{II} B_{ni} \sin(\omega_{ni}\tau) \right], \quad (56)$$

$$\bar{w}_2(\xi, \tau) = \sum_{n=1}^{\infty} \sin(n\pi\xi) \left[A_{nII} \sin(\Omega\tau) + \sum_{i=1}^{II} \alpha_{ni} B_{ni} \sin(\omega_{ni}\tau) \right], \quad (57)$$

where

$$A_{nI} = \lambda_1 \left[\frac{\alpha_{nII}}{(\omega_{nI}^2 - \Omega^2)} - \frac{\alpha_{nI}}{(\omega_{nII}^2 - \Omega^2)} \right], \quad (58)$$

$$A_{nII} = \lambda_1 \alpha_{nI} \alpha_{nII} \left[\frac{1}{(\omega_{nI}^2 - \Omega^2)} - \frac{1}{(\omega_{nII}^2 - \Omega^2)} \right], \quad (59)$$

$$B_{nI} = -\lambda_1 \Omega \alpha_{nII} \frac{1}{\omega_{nI}} \cdot \frac{1}{(\omega_{nI}^2 - \Omega^2)}, \quad (60)$$

$$B_{nII} = \lambda_1 \Omega \alpha_{nI} \frac{1}{\omega_{nII}} \cdot \frac{1}{(\omega_{nII}^2 - \Omega^2)}, \quad (61)$$

$$\lambda_1 = \frac{4Mr}{n\pi(\alpha_{nII} - \alpha_{nI})} \quad \text{and} \quad M = \frac{1}{1 + \eta^2 k_n^2}. \quad (62)$$

It can be noticed that equations (56) and (57) consist of two parts. The first part, containing the term $\sin(\Omega\tau)$, represents the steady-state forced vibrations of the SWCNT system, while the second part,

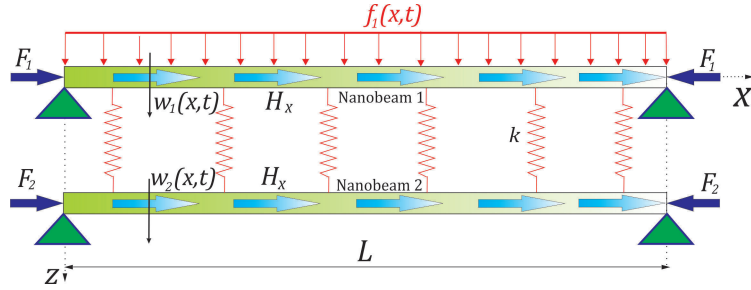


Figure 2. The double nanobeam system coupled by the Winkler elastic medium subjected to the uniformly distributed harmonic load.

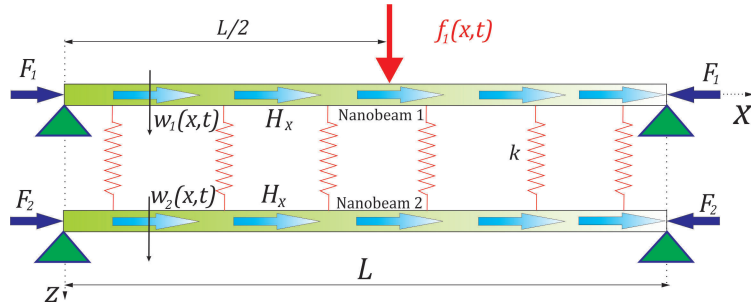


Figure 3. The double nanobeam system coupled by the Winkler elastic medium subjected to the concentrated harmonic force.

involving the terms $\sin(\omega\tau)$, denotes the free vibration of the SWCNT system. Assuming that only the steady-state response has practical significance, and ignoring the free response, the forced vibrations of the SWCNT system can be obtained by

$$\bar{w}_1(\xi, \tau) = \sin(\Omega\tau) \sum_{n=1}^{\infty} A_{nI} \sin(n\pi\xi), \tag{63}$$

$$\bar{w}_2(\xi, \tau) = \sin(\Omega\tau) \sum_{n=1}^{\infty} A_{nII} \sin(n\pi\xi), \tag{64}$$

where A_{nI} and A_{nII} denote the steady-state vibration amplitudes of the two nanobeams, respectively.

3.2.2. Concentrated harmonic force. The concentrated harmonic force

$$\bar{f}_1(\xi, \tau) = r \sin(\Omega\tau) \delta\left(\xi - \frac{1}{2}\right) \tag{65}$$

acts at the middle of the SWCNT system (see Figure 3), where r is the amplitude and Ω is the frequency of the exciting harmonic force and $\delta(\xi)$ is the Dirac delta function.

By substituting (65) into equations (51) and (52), we obtain

$$R_{nI} = 2Mr \frac{\alpha_{nII}}{\alpha_{nII} - \alpha_{nI}} \sin\left(\frac{1}{2}n\pi\right) \sin(\Omega\tau)[1 + \eta^2 k_n^2], \quad (66)$$

$$R_{nII} = 2Mr \frac{\alpha_{nI}}{\alpha_{nI} - \alpha_{nII}} \sin\left(\frac{1}{2}n\pi\right) \sin(\Omega\tau)[1 + \eta^2 k_n^2]. \quad (67)$$

The introduction of (66) and (67) into (49) and (50) gives

$$\bar{w}_1(\xi, \tau) = \sum_{n=1}^{\infty} \sin(n\pi\xi) \left[A_{nI} \sin(\Omega\tau) + \sum_{i=I}^{II} B_{ni} \sin(\omega_{ni}\tau) \right], \quad (68)$$

$$\bar{w}_2(\xi, \tau) = \sum_{n=1}^{\infty} \sin(n\pi\xi) \left[A_{nII} \sin(\Omega\tau) + \sum_{i=I}^{II} \alpha_{ni} B_{ni} \sin(\omega_{ni}\tau) \right], \quad (69)$$

where

$$A_{nI} = \lambda_2 \left[\frac{\alpha_{nII}}{(\omega_{nI}^2 - \Omega^2)} - \frac{\alpha_{nI}}{(\omega_{nII}^2 - \Omega^2)} \right], \quad (70)$$

$$A_{nII} = \lambda_2 \alpha_{nI} \alpha_{nII} \left[\frac{1}{(\omega_{nI}^2 - \Omega^2)} - \frac{1}{(\omega_{nII}^2 - \Omega^2)} \right], \quad (71)$$

$$B_{nI} = -\lambda_2 \Omega \alpha_{nII} \frac{1}{\omega_{nI}} \cdot \frac{1}{(\omega_{nI}^2 - \Omega^2)}, \quad (72)$$

$$B_{nII} = \lambda_2 \Omega \alpha_{nI} \frac{1}{\omega_{nII}} \cdot \frac{1}{(\omega_{nII}^2 - \Omega^2)}, \quad (73)$$

$$M = \frac{1}{1 + \eta^2 k_n^2} \quad \text{and} \quad \lambda_2 = \frac{2rM(1 + n^2\pi^2\eta^2)}{(\alpha_{nII} - \alpha_{nI})} \sin\left(\frac{1}{2}n\pi\right) = \frac{2r}{(\alpha_{nII} - \alpha_{nI})} \sin\left(\frac{1}{2}n\pi\right), \quad (74)$$

It can be noticed that equations (68) and (69) consist of two parts described in Section 3.2.1. Assuming that only the steady-state response has practical significance, and ignoring the free response, the forced vibrations of the SWCNT system can be obtained by relations (63) and (64).

3.2.3. Moving constant force F . The moving loads with constant force $F(\tau) = F$ and

$$\bar{f}_1(\xi, \tau) = F\delta(\xi - v\tau) \quad (75)$$

act upon the SWCNT system (see Figure 4), where F is the magnitude of a constant force and $\delta(\xi)$ is the Dirac delta function. By substituting (75) into (51) and (52), we obtain

$$R_{nI} = 2MF \frac{\alpha_{nII}}{\alpha_{nII} - \alpha_{nI}} \sin(n\pi v\tau)[1 + \eta^2 k_n^2], \quad n = 1, 3, 5, \dots, \quad (76)$$

$$R_{nII} = 2MF \frac{\alpha_{nI}}{\alpha_{nI} - \alpha_{nII}} \sin(n\pi v\tau)[1 + \eta^2 k_n^2], \quad n = 1, 3, 5, \dots \quad (77)$$

The introduction of (76) and (77) into (49) and (50) gives

$$\bar{w}_1(\xi, \tau) = \sum_{n=1}^{\infty} \sin(n\pi\xi) \left[A_{nI} \sin(\Omega_n \tau) + \sum_{i=I}^{\text{II}} B_{ni} \sin(\omega_{ni} \tau) \right], \quad (78)$$

$$\bar{w}_2(\xi, \tau) = \sum_{n=1}^{\infty} \sin(n\pi\xi) \left[A_{n\text{II}} \sin(\Omega_n \tau) + \sum_{i=I}^{\text{II}} \alpha_{ni} B_{ni} \sin(\omega_{ni} \tau) \right], \quad (79)$$

where

$$A_{nI} = \lambda_3 \left[\frac{\alpha_{n\text{II}}}{\omega_{nI}^2 - \Omega_n^2} - \frac{\alpha_{nI}}{\omega_{n\text{II}}^2 - \Omega_n^2} \right], \quad (80)$$

$$A_{n\text{II}} = \lambda_3 \alpha_{nI} \alpha_{n\text{II}} \left[\frac{1}{\omega_{nI}^2 - \Omega_n^2} - \frac{1}{\omega_{n\text{II}}^2 - \Omega_n^2} \right], \quad (81)$$

$$B_{nI} = -\lambda_3 \Omega_n \alpha_{n\text{II}} \frac{1}{\omega_{nI}} \cdot \frac{1}{(\omega_{nI}^2 - \Omega_n^2)}, \quad (82)$$

$$B_{n\text{II}} = \lambda_3 \Omega_n \alpha_{nI} \frac{1}{\omega_{n\text{II}}} \cdot \frac{1}{(\omega_{n\text{II}}^2 - \Omega_n^2)}, \quad (83)$$

$$\lambda_3 = \frac{2FM(1 + \eta^2 k_n^2)}{(\alpha_{n\text{II}} - \alpha_{nI})} = \frac{2F}{(\alpha_{n\text{II}} - \alpha_{nI})}, \quad (84)$$

$$\Omega_n = n\pi v = k_n v, \quad n = 1, 3, 5, \dots \quad (85)$$

It can be noticed that equations (78) and (79) consist of two parts described in Section 3.2.1. Assuming that only the steady-state response has practical significance, and ignoring the free response, the forced vibrations of the SWCNT system can be obtained by

$$\bar{w}_1(\xi, \tau) = \sin(\Omega_n \tau) \sum_{n=1}^{\infty} A_{nI} \sin(n\pi\xi), \quad (86)$$

$$\bar{w}_2(\xi, \tau) = \sin(\Omega_n \tau) \sum_{n=1}^{\infty} A_{n\text{II}} \sin(n\pi\xi), \quad (87)$$

where A_{nI} and $A_{n\text{II}}$ denote the steady-state vibration amplitudes of the two nanobeams, respectively.

3.2.4. Moving concentrated harmonic force. The moving loads with harmonic concentrated force $F(\tau) = F \sin(\Omega\tau)$ and

$$\bar{f}_1(\xi, \tau) = F \sin(\Omega\tau) \delta(\xi - v\tau) \quad (88)$$

acts upon the SWCNT system (see Figure 4), where F is the amplitude and Ω is the frequency of the harmonic force. By substituting (88) into (51) and (52), we obtain

$$R_{nI} = 2MF \frac{\alpha_{n\text{II}}}{\alpha_{n\text{II}} - \alpha_{nI}} \sin(\Omega\tau) \sin(n\pi v\tau) [1 + \eta^2 k_n^2], \quad (89)$$

$$R_{n\text{II}} = 2MF \frac{\alpha_{nI}}{\alpha_{nI} - \alpha_{n\text{II}}} \sin(\Omega\tau) \sin(n\pi v\tau) [1 + \eta^2 k_n^2]. \quad (90)$$

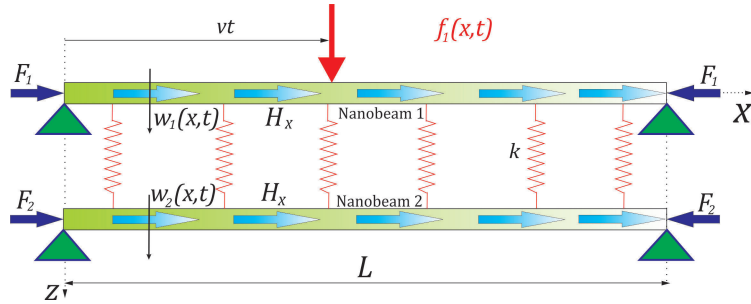


Figure 4. The double nanobeam system coupled by the Winkler elastic medium subjected to the moving concentrated force.

The introduction of (89) and (90) into (49) and (50) gives

$$\bar{w}_1(\xi, \tau) = \sum_{n=1}^{\infty} \sin(n\pi\xi) \left[A_{nI} \sin(\Omega_n \tau) \sin(\Omega \tau) + B_{nI} \cos(\Omega_n \tau) \cos(\Omega \tau) + \sum_{i=I}^{II} C_{ni} \cos(\omega_{ni} \tau) \right], \quad (91)$$

$$\bar{w}_2(\xi, \tau) = \sum_{n=1}^{\infty} \sin(n\pi\xi) \left[A_{nII} \sin(\Omega_n \tau) \sin(\Omega \tau) + B_{nII} \cos(\Omega_n \tau) \cos(\Omega \tau) + \sum_{i=I}^{II} \alpha_{ni} C_{ni} \cos(\omega_{ni} \tau) \right], \quad (92)$$

where

$$A_{nI} = \lambda_4 \left[\frac{\alpha_{nII} u_{nI}}{n_{nI} m_{nI}} - \frac{\alpha_{nI} u_{nII}}{n_{nII} m_{nII}} \right], \quad (93)$$

$$A_{nII} = \lambda_4 \alpha_{nI} \alpha_{nII} \left[\frac{u_{nI}}{n_{nI} m_{nI}} - \frac{u_{nII}}{n_{nII} m_{nII}} \right], \quad (94)$$

$$B_{nI} = 2\lambda_4 \Omega_n \Omega \left[\frac{\alpha_{nI}}{n_{nII} m_{nII}} - \frac{\alpha_{nII}}{n_{nI} m_{nI}} \right], \quad (95)$$

$$B_{nII} = 2\lambda_4 \Omega_n \Omega \alpha_{nI} \alpha_{nII} \left[\frac{1}{n_{nII} m_{nII}} - \frac{1}{n_{nI} m_{nI}} \right], \quad (96)$$

$$C_{nI} = \frac{2\lambda_4 \Omega_n \Omega \alpha_{nII}}{n_{nI} m_{nI}}, \quad (97)$$

$$C_{nII} = -\frac{2\lambda_4 \Omega_n \Omega \alpha_{nI}}{n_{nII} m_{nII}}, \quad (98)$$

$$\lambda_4 = \frac{2FM(1 + \eta^2 k_n^2)}{(\alpha_{nII} - \alpha_{nI})} = \frac{2F}{(\alpha_{nII} - \alpha_{nI})}, \quad (99)$$

$$\Omega_n = n\pi v = k_n v, \quad (100)$$

$$m_{ni} = \omega_{ni}^2 - (\Omega_n - \Omega)^2, \quad (101)$$

$$n_{ni} = \omega_{ni}^2 - (\Omega_n + \Omega)^2, \quad (102)$$

$$u_{ni} = \omega_{ni}^2 - \Omega_n^2 - \Omega^2, \quad i = I, II. \quad (103)$$

It can be noticed that equations (91) and (92) consist of three parts. Assuming that only the steady-state response has practical significance, and ignoring the free response, the forced vibrations of the SWCNT system can be obtained by

$$\bar{w}_1(\xi, \tau) = \sum_{n=1}^{\infty} \sin(n\pi\xi) [A_{nI} \sin(\Omega_n \tau) \sin(\phi\tau) + B_{nI} \cos(\Omega_n \tau) \cos(\Omega\tau)], \quad (104)$$

$$\bar{w}_2(\xi, \tau) = \sum_{n=1}^{\infty} \sin(n\pi\xi) [A_{nII} \sin(\Omega_n \tau) \sin(\phi\tau) + B_{nII} \cos(\Omega_n \tau) \cos(\Omega\tau)], \quad (105)$$

where A_{nI} and A_{nII} and B_{nI} and B_{nII} denote the steady-state vibration amplitudes of the two nanobeams, respectively. In this paper we will analyze only A_{nI} and A_{nII} steady-state vibration amplitudes.

4. Comparative study and numerical results

The presented methodology for the analyzed forced response of the double nanobeam system coupled by the elastic medium based on the nonlocal elasticity theory can be applied for the forced transversal vibration analysis of coupled carbon nanotubes, ZnO nanotubes, boron-nitride nanobeams and other magnetically affected nanomaterials [Barone and Peralta 2008; Kumar and Mohammad 2011]. Also, the Winkler elastic layer may represent some interatomic forces between two nanotubes, such as van der Waals interaction [Ru 2001]. We present a comparative study of the analytical results obtained in this paper and the results found in the literature.

This section is divided into three parts. In the first part, the fundamental frequency of the first nanobeam is compared with [Şimşek 2010b] and implemented via the MD simulation of vibrational response of the SWCNT according to Ansari and Sahmani [2012] and Ansari et al. [2012]. In the second part, the obtained numerical results for the ratio of the steady-state vibration amplitude of the double nanobeam system influenced by the axial magnetic field are compared with the results obtained by the scale-free structural theory proposed by Zhang et al. [2008], who analyzed the forced response of an axially compressed double beam system using the classical elasticity theory where the influence of the magnetic field was neglected. The third part discusses the influence of small scale and the axial magnetic field on the forced response of the double nanobeam system.

4.1. Fundamental frequency results. In this section, the natural frequency of the first nanobeam is compared with [Şimşek 2010b]. For DSWCNT it is well known that the lowest natural frequency and buckling load of such a system represents the fundamental frequency and critical buckling load and it is independent of the influence of the number of nanobeams in the system and chain coupling conditions; see [Karličić et al. 2014b; 2014a]. Fundamental frequency and critical buckling load are equivalent to the natural frequency and buckling load of a single nanobeam. The following parameters are used in computing the numerical results: $E = 1$ TPa, $\rho = 2300$ kg/m³, $d = 1$ nm, $t_b = 0.35$ nm [Şimşek 2010b]. The length of the nanotube is taken as variable for the various values of the aspect ratio L/d . The parameter e_0 was estimated as $e_0 = (\pi^2 - 4)^{1/2}/2\pi \cong 0.39$ by Eringen [1983]. Therefore, in this study, the nonlocal parameter μ is taken as 0, 1, 2, 3, 4.

Excellent agreement between the present frequencies and those of [Şimşek 2010b] can be observed from Table 1. It is shown that inclusion of the nonlocal parameter μ decreases the frequencies of the

L/d	μ	$\bar{\omega}_{ni}^0$			
		Şimşek [2010b]	Present study (MP = 0)	Present study (MP = 10)	Present study (MP = 20)
10	0	9.8696	9.8696	11.3501	12.6586
	1	9.4158	9.4158	10.9578	12.3081
	2	9.0194	9.0194	10.6191	12.0076
	3	8.6692	8.6692	10.3233	11.7468
	4	8.3569	8.3569	10.0625	11.5182
20	0	9.8696	9.8696	11.3501	12.6586
	1	9.7501	9.7501	11.2463	12.5656
	2	9.6347	9.6347	11.1464	12.4763
	3	9.5234	9.5234	11.0504	12.3906
	4	9.4158	9.4158	10.9578	12.3081
50	0	9.8696	9.8696	11.3501	12.6586
	1	9.8501	9.8501	11.3332	12.6435
	2	9.8308	9.8308	11.3164	12.6285
	3	9.8116	9.8116	11.2998	12.6135
	4	9.7925	9.7925	11.2832	12.5987

Table 1. Comparison of the nondimensional frequencies from Equation (111) for the simply supported nanobeam.

nanobeam 1. It is seen that the effect of the magnetic field (MP = 10, 20) is to increase frequencies of SWCNT. When the value of L/d is increased, the effect of the nonlocal parameter μ on the frequencies decreases.

Without loss of generality, we assume

$$\bar{F}_2 = \chi \bar{F}_1, \quad 0 \leq \chi \leq 1. \tag{106}$$

Based on (106), we obtain the same form of natural frequencies for (28) and (29) with different coefficients b_1 and c_1 :

$$\bar{\omega}_{ni}^2 = \frac{1}{2} [b \mp \sqrt{b^2 - 4c}], \quad i = \text{I, II}, \tag{107}$$

where

$$b_1 = 2K - (\chi + 1)\bar{F}_1 k_n^2 + 2MPk_n^2 + 2\frac{k_n^4}{1 + \eta^2 k_n^2}, \tag{108}$$

$$c_1 = \left[K - (\bar{F}_1 - \text{MP})k_n^2 + \frac{k_n^4}{1 + \eta^2 k_n^2} \right] \left[K - (\chi \bar{F}_1 - \text{MP})k_n^2 + \frac{k_n^4}{1 + \eta^2 k_n^2} \right] - K^2. \tag{109}$$

By substituting the new expressions (107) for natural frequencies into (33) and (34), we obtain the new expressions for the amplitude as

$$\bar{\alpha}_{ni} = \frac{K - (\bar{F}_1 - \text{MP})k_n^2 + \frac{k_n^4}{1 + \eta^2 k_n^2} - \bar{\omega}_{ni}^2}{K}, \quad i = \text{I, II}. \tag{110}$$

When the axial compression is absent, we obtain

$$(\bar{\omega}_{nI}^0)^2 = \frac{k_n^4}{1 + \eta^2 k_n^2} + k_n^2 M P, \quad (111)$$

$$(\bar{\omega}_{nII}^0)^2 = 2K + \frac{k_n^4}{1 + \eta^2 k_n^2} + k_n^2 M P, \quad (112)$$

$$\bar{\alpha}_{nI}^0 = 1, \quad \bar{\alpha}_{nII}^0 = -1. \quad (113)$$

To determine the effect of the axial compressive load and magnetic field on the steady-state vibration amplitudes A_{nI} and A_{nII} of the system and also for the comparative study, we define the ratio of the steady-state vibration amplitudes as

$$\psi_1 = \frac{A_{nI}}{A_{nI}^0}, \quad \psi_2 = \frac{A_{nII}}{A_{nII}^0}, \quad (114)$$

where A_{nI}^0 and A_{nII}^0 are the steady-state vibration amplitudes of the two beams without axial compression. We then introduce the ratio of the axial compressive force and critical buckling load as

$$p = \frac{\bar{F}}{P_{cr}}, \quad (115)$$

with

$$P_{cr} = \frac{\pi^2}{1 + \eta^2 \pi^2}, \quad (116)$$

where P_{cr} is the nonlocal critical buckling load, which is the smallest load at which a single nanobeam ceases to be in stable equilibrium under axial compression. From (27) it follows that

$$\bar{F} = \frac{k_n^2}{1 + \eta^2 k_n^2}. \quad (117)$$

By substituting the dimensionless \bar{F} from (16) we can write

$$P_{cr} = \frac{1}{1 + \eta^2 \pi^2} E I \frac{\pi^2}{L^2}. \quad (118)$$

For $\eta = 0$, namely for an ordinary beam,

$$P_{cr} = E I \frac{\pi^2}{L^2}, \quad (119)$$

where P_{cr} is known as the Euler load, which is the smallest load at which a single beam ceases to be in stable equilibrium under axial compression [Zhang et al. 2008].

4.1.1. Molecular dynamics simulation results. In order to justify the accuracy of this paper, it is necessary to implement the MD simulation of vibrational response of the SWCNT. Molecular dynamics (MD) simulation is an atomistic method for analysis of different nanostructures. Through the fast development of various fields of nanotechnology, MD simulation has been considered as a powerful and accurate implement to study of systems at nanoscale, according to Ansari et al. [2012]. Without introducing the

L/d	MD simulation [Ansari et al. 2012]	Present study ($\eta H_x^2 = 0$)	Present study ($\eta H_x^2 > 0$)
8.3	0.5299	0.5485	0.8284
10.1	0.3618	0.3707	0.6306
13.7	0.1931	0.2016	0.4267
17.3	0.1103	0.1264	0.3236
20.9	0.0724	0.0860	0.2613
24.5	0.0519	0.0630	0.2195
28.1	0.0425	0.0479	0.1895
31.6	0.0358	0.0379	0.1674
35.3	0.0287	0.0303	0.1491
39.1	0.0259	0.0247	0.1341

Table 2. Fundamental frequencies (THz) for (8, 8) armchair SWCNT obtained from MD simulations of Euler–Bernoulli beam models, $R/l = 3$, $l = \mu^{1/2}$, $H_x = 1 \cdot 10^8$ A/m, $\eta = 4\pi \cdot 10^{-7}$.

dimensionless expression (16), the fundamental frequency of the first nanobeam is presented in the form

$$\omega_{n1} = \sqrt{\frac{\eta H_x^2}{\rho} (n\pi/L)^2 + \frac{EI(n\pi/L)^4}{\rho A(1 + \mu(n\pi/L)^2)}}. \quad (120)$$

Authors have found MD simulation results for vibration and buckling of a single-layer graphene sheet presented by Ansari and Sahmani [2012] and Ansari et al. [2012]. Thus, our results for the lowest natural frequency of DSWCNT can be used to validate them with the results obtained for the free vibration of a SWCNT via molecular dynamics simulation in [Ansari and Sahmani 2012] and [Ansari et al. 2012].

In the current study, the effective thickness of the SWCNTs is assumed to be equal to the spacing of graphite, $h = 0.34$ nm, radius of the nanotubes is $R = d/2$, where d is diameter of the SWCNT [Ansari et al. 2012]. The Poisson's ratio $\nu = 0.3$, Young's modulus $E = 1.1$ TPa and mass density $\rho = 2300$ kg/m³ are considered in the analysis. To validate the present approach, MD simulations are conducted for a simply supported (8, 8) armchair SWCNT with different aspect ratios ranging from 8.3 to 39.1. Table 2 present the values of fundamental frequency obtained from MD simulations and also the Euler–Bernoulli beam models based on the nonlocal elastic theory. The results predicted by the present models are found to be in excellent agreement with the ones obtained from MD simulation, which indicates the capability of the present approach to accurately predict frequencies of SWCNT. From Table 2, the frequency of SWCNT is decreasing with increasing length-to-diameter ratio.

It can be noticed that the results obtained by using the Bernoulli–Fourier method, when is $\eta H_x^2 = 0$, are in agreement with the results presented by Ansari and Sahmani [2012] and Ansari et al. [2012]. Between these values there is a very little variation because we neglected moment of inertia. Taking into account the value of magnetic field permeability η and axial magnetic field H_x from [Murmu et al. 2012b], as expected, the values of frequency of SWCNT are greater than the values from [Ansari and Sahmani 2012] and [Ansari et al. 2012].

4.2. Steady-state amplitudes results of the DSWCNT system. In the second part, to validate the results obtained for the steady-state vibration amplitude we adopt the values for material characteristics from [Zhang et al. 2008], where $E = 10^{10}$ [Pa] is the elastic modulus, $I = 4 * 10^{-4}$ [m⁴] is the moment of inertia, $L = 10$ [m] is the length of beam, and $K = 2 * 10^5$ [N/m²] is the stiffness coefficient of the elastic medium. The results obtained by the classical and nonlocal theories are comparable in the case when the results are given in the dimensionless form. Since the steady-state vibration amplitude is expressed in dimensionless form here, it is possible to compare these results with the results obtained in [Zhang et al. 2008]. It should be noted that the validation of the obtained results was conducted for cases of uniform and concentrated harmonic load, and excellent agreement is shown with the results proposed by Zhang et al. [2008].

In order to compare the obtained results for the ratio of the steady-state amplitudes for the case of the uniformly distributed harmonic load, we determine the steady-state vibration amplitudes (A_{nI} and A_{nII}) and (A_{nI}^0 and A_{nII}^0) by substituting equations (107)–(110) and (111)–(113) into equations (58) and (59), respectively. For the vibration mode number $n = 3$ and the exciting frequency $\Omega = 0.6\omega_{nII}$, the variation of the steady-state amplitude ratios ψ_1 and ψ_2 with a change in the axial force ratio for different values of axial magnetic fields is shown in Figure 5. It can be observed that the steady-state amplitude ratios ψ_1 and ψ_2 increase with an increase in the axial compressive load, which leads to an increase in the steady-state amplitudes A_{nI} and A_{nII} of DNBS. Moreover, it can be noticed that the axial compression ratio χ has negligible effects on the first steady-state amplitude ratio ψ_1 , but a significant influence on the second steady-state amplitude ratio ψ_2 . Also, decreasing the axial compression ratio χ causes an obvious reduction of the second steady-state amplitude A_{nII} . It is clear from Figure 5 that larger values of the amplitude of the axial magnetic field lead to a reduction in the ratios ψ_1 and ψ_2 , which implies that the amplitudes of the steady-state vibrations A_{nI} and A_{nII} also decrease. However, from the physical point of view, the axial magnetic field leads to an increase in the overall stiffness and thereby to an increase in the natural frequencies of the system. This effect allows us the practical application of such a system, because it is possible to change the natural frequencies ω_{nI} and ω_{nII} and the steady-state amplitudes A_{nI} and A_{nII} without changing any other material and geometric parameters of the DNBS. It should be noted that when the intensity of the axial magnetic field and nonlocal parameter are equal to zero, the nonlocal double nanobeam system is reduced to the classical double beam system analyzed in [Zhang et al. 2008]. The results for ratios ψ_1 and ψ_2 obtained in the case when $MP = 0$ and $\eta = 0$ are also shown in Figure 5. The comparative study for the case of the concentrated harmonic force is also carried out in a similar manner. The analysis of the obtained results for the ratios ψ_1 and ψ_2 shows that we get exactly the same results as in the case of the continuous uniformly distributed load. The results obtained in this study are in line with the results obtained in [Zhang et al. 2008].

In the following part of the comparative study we provide an analysis of the steady-state amplitude ratios ψ_1 and ψ_2 for the cases of the uniformly distributed load (Figures 5 and 6), and the moving concentrated harmonic force (Figures 7 and 8). The dimensionless parameters of the coupled DNBS which are used in numerical simulations in Figures 6, 7 and 8 are: $K = 50$, $\chi = 0.5$, $\xi = 0.5$, $\nu = 0.3$ and $n = 1$. As already mentioned, the results obtained for the steady-state amplitude ratio in the case of the harmonic concentrated load are identical with the results obtained for the first case of excitation, while the case of the moving constant force represents only a special case of the moving harmonic concentrated force.

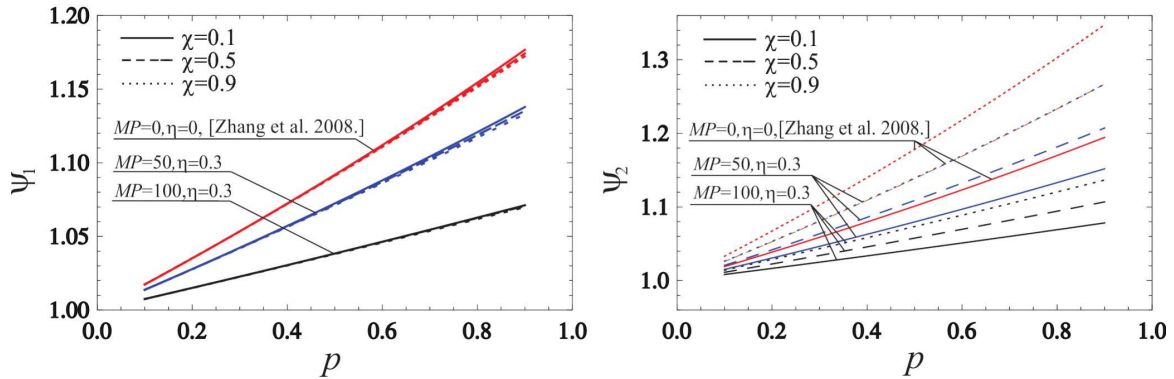


Figure 5. The relationship between the dimensionless parameter $p = \bar{F}/P_{cr}$ and (left) the ratio $\psi_1 = A_{nI}/A_{nI}^0$ and (right) the ratio $\psi_2 = A_{nII}/A_{nII}^0$, for different axial compression ratios χ and magnetic fields MP in the case of a uniformly distributed load.

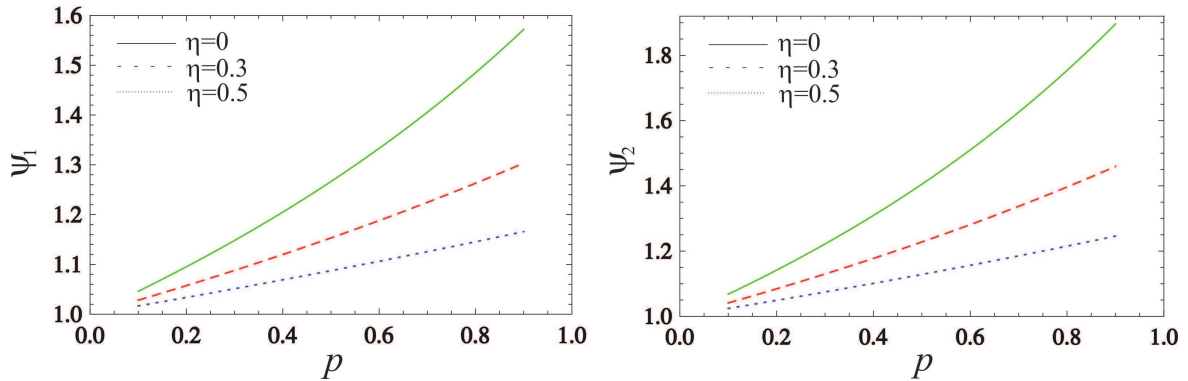


Figure 6. The relationship between the dimensionless parameter $p = \bar{F}/P_{cr}$ and (left) the ratio $\psi_1 = A_{nI}/A_{nI}^0$ and (right) the ratio $\psi_2 = A_{nII}/A_{nII}^0$ for different nonlocal parameters η in the case of a uniformly distributed load.

Figure 6 shows the relationship between the ratios ψ_1 and ψ_2 in the case of the uniformly distributed load, and the dimensionless parameter $p = \bar{F}/P_{cr}$ in the range 0–1 for different nonlocal parameters η . From these figures, the ratios ψ_1 and ψ_2 decrease with an increase in the nonlocal parameter η , which implies that the magnitudes of the steady-state vibration amplitudes A_{nI} and A_{nII} get smaller when the nonlocal parameter η becomes larger. Also, it is interesting to note that from the physical point of view the nonlocal parameter has dampening effects on the steady-state vibration amplitudes. In addition, an increase in the ratio p leads to an increase in both steady-state amplitude ratios ψ_1 and ψ_2 in a similar manner. So from the physical point of view, it can be concluded that the overall stiffness of the system decreases with the increase in the ratio p .

Figures 7 and 8 show the influence of the longitudinal magnetic field MP and the nonlocal parameter η on the relationship between the ratios ψ_1 and ψ_2 , and ratio $p = \bar{F}/P_{cr}$ in the range 0–1 in the case of the moving harmonic concentrated force, respectively. From these figures we can see that the steady-state vibration amplitude ratios ψ_1 and ψ_2 decrease with the increase in the parameter of the magnetic field

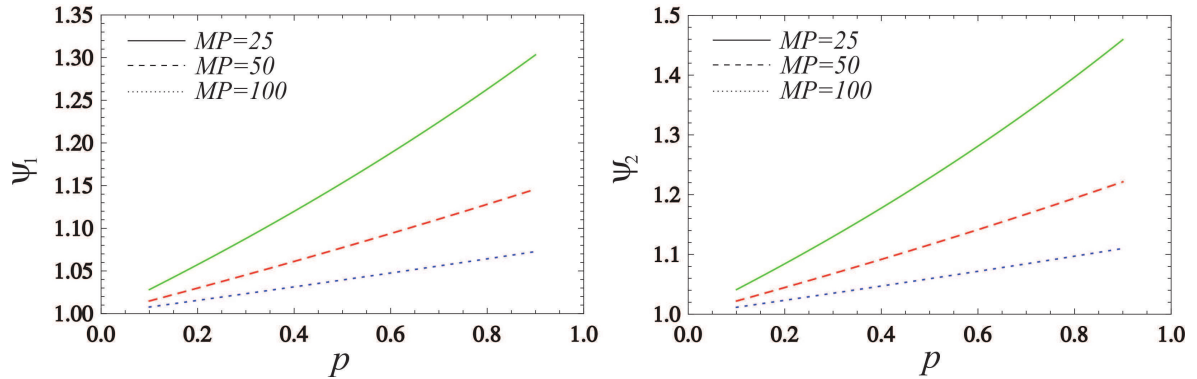


Figure 7. The relationship between the dimensionless parameter $p = \bar{F}/P_{cr}$ and (left) the ratio $\psi_1 = A_{nI}/A_{nI}^0$ and (right) the ratio $\psi_2 = A_{nII}/A_{nII}^0$ for different axial magnetic fields MP in the case of a moving concentrated harmonic force.

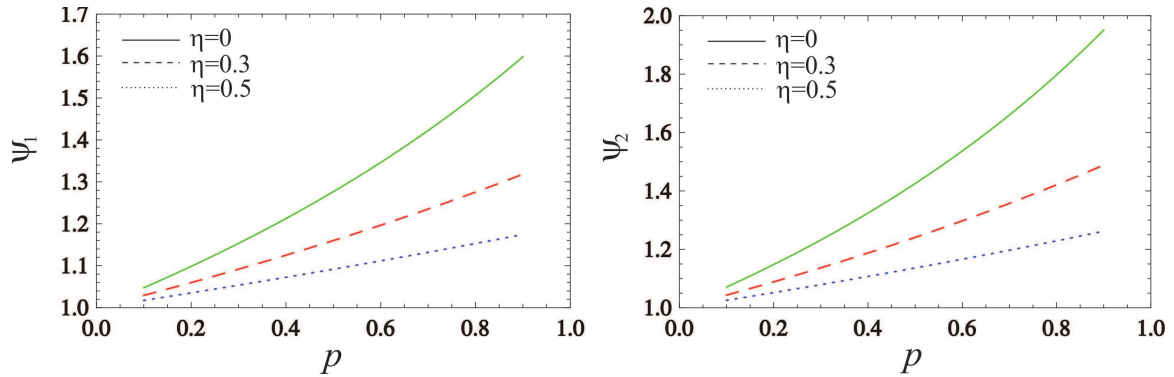


Figure 8. The relationship between the dimensionless parameter $p = \bar{F}/P_{cr}$ and (left) the ratio $\psi_1 = A_{nI}/A_{nI}^0$ and (right) the ratio $\psi_2 = A_{nII}/A_{nII}^0$ for different nonlocal parameters η in the case of a moving concentrated harmonic force.

and nonlocality η . This implies that the magnitudes of the steady-state vibration amplitudes A_{nI} and A_{nII} act in a similar manner to the case of the uniform harmonic excitation. It is interesting to note that values for the steady-state amplitude ratio are higher for the moving harmonic load than for the uniform harmonic loads. However, from the physical point of view, it can be noted that the speed of the moving load significantly affects the value of the steady-state vibration amplitudes A_{nI} and A_{nII} of the coupled nanobeams. The present results for the ratio of amplitudes are consistent with the results found in the literature [Zhang et al. 2008].

In order to compare the results of the presented study with those in the existing study by Zhang et al. [2008], the values of the steady-state vibration amplitude ratios ψ_1 and ψ_2 for the uniformly distributed harmonic load and the concentrated harmonic force are represented in Table 3. It is found that the ratios ψ_1 and ψ_2 in this case are totally the same. From the presented data we can conclude that the influence of the longitudinal magnetic field MP and the nonlocal parameter η on the relationship between ratio ψ_1 and ψ_2 causes a decrease in their values, as shown in the above figures.

[Zhang et al. 2008]			
MP	η	$\psi_1 = A_{nI}/A_{nI}^0$	$\psi_2 = A_{nII}/A_{nII}^0$
0	0	1.1965	1.3019
50	0.3	1.1499	1.2277
50	0.5	1.0872	1.1309
100	0.3	1.0779	1.1175
100	0.5	1.0436	1.0658

Table 3. Analytical validation of the steady-state vibration amplitude ratios ψ_1 and ψ_2 . Here $\chi = 0.5$.

4.3. Forced vibration response. In this subsection, forced vibration responses at the nanobeams mid-points are analyzed for two cases of external excitation under the influence of the longitudinal magnetic field within the framework of the nonlocal elasticity theory. In the first case we consider that the uniform harmonic load acts on the first nanobeam in the DNBS (Figure 2) while in the second one we consider the moving harmonic concentrated force (Figure 4). Also, we assume that both nanobeams in the DNBS have the same geometric and material characteristics and are subjected to the axial compressive loads \bar{F}_1 and \bar{F}_2 . By using the analytical solution for transversal displacements obtained for these two particular cases of external excitation, we plot $\bar{w}_1(\xi, \tau)$ and $\bar{w}_2(\xi, \tau)$ as functions of time for different nonlocal and magnetic field parameters, as shown in Figures 9–12.

To analyze forced vibrations, we use smaller values for the dimensionless stiffness modulus K and magnetic fields MP, because using larger values leads to obtaining very smaller values for the vibration amplitude of transversal displacements $\bar{w}_1(0.5, \tau)$ and $\bar{w}_2(0.5, \tau)$. The following dimensionless parameters of the coupled DNBS are used here in the numerical simulations: $K = 5$, $\chi = 0.5$, $\bar{F}_1 = 0.2$, $\xi = 0.5$, and $n = 1$, where the exciting frequency is $\Omega = 0.6\omega_{nII}$. It can be observed that the axial magnetic field diminishes the amplitudes of transversal vibration $\bar{w}_1(\xi, \tau)$ and $\bar{w}_2(\xi, \tau)$ in both cases of external excitation. Moreover, this effect allows us to change the stiffness of the carbon nanotubes and therefore change the overall stiffness of the DNBS. However, changing the stiffness of the system leads to changes in the natural frequency of the system, so it is possible to avoid the resonance region for different cases of external excitation [Karličić et al. 2014c]. Furthermore, by carefully selecting the intensity of the magnetic field we can set the response vibration amplitude in a certain range without changing any other material and geometric characteristics of the DNBS. This fact has significance in practical applications for the control of vibration amplitude in the NEMS and nanocomposite structures based on the CNTs. Also, these figures show how the coupled DNBS responds to changes in the nonlocal parameter η for different cases of external excitation. It can be noticed that the nonlocal parameter has a dampening effect on both response vibration amplitudes of the DNBS, but in the case of the moving harmonic concentrated force we observe a larger effect on the vibration amplitude. This means that the effect of nonlocality causes a larger reduction of the vibration amplitude of transversal displacements $\bar{w}_1(0.5, \tau)$ and $\bar{w}_2(0.5, \tau)$ than in the first case of external excitation.

The presented work shows the possibility to control vibration amplitudes and natural frequencies in a certain range by changing only the external magnetic field parameter without changing any other physical parameter of the DNBS. Also, this ability provides us with a great practical application of such systems

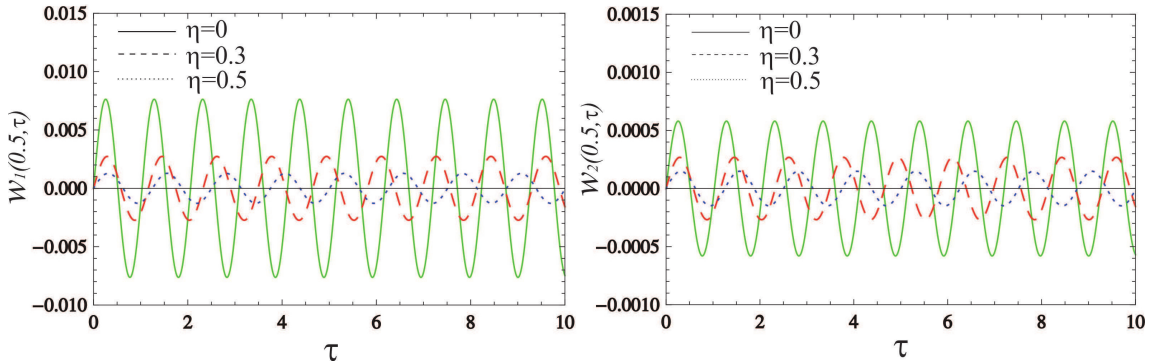


Figure 9. The relationship between forced vibrations $\bar{w}_1(0.5, \tau)$ (left) and $\bar{w}_2(0.5, \tau)$ (right) and dimensionless time for different nonlocal parameters η in the case of the uniformly distributed harmonic load.

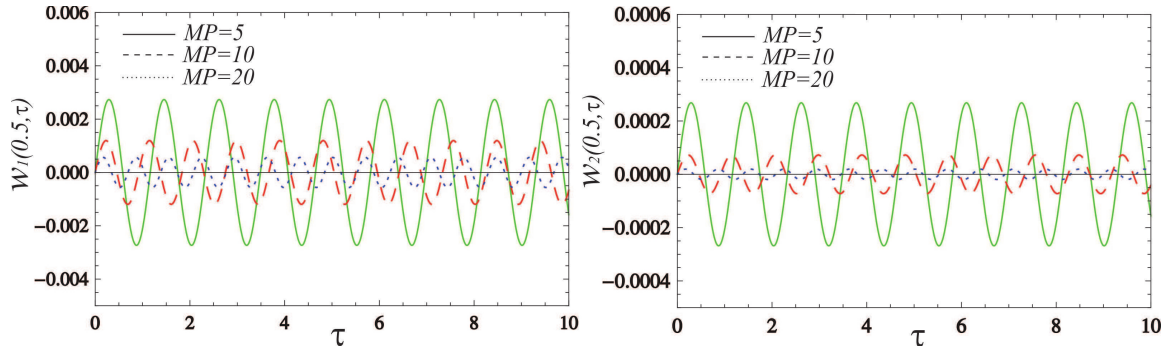


Figure 10. The relationship between forced vibrations $\bar{w}_1(0.5, \tau)$ (left) and $\bar{w}_2(0.5, \tau)$ (right) and dimensionless time for different axial magnetic fields MP in the case of the uniformly distributed harmonic load.

in dynamic absorbers, nanoresonators and nanoactuator devices. It should be noted that the longitudinal magnetic field can be considered analogous to a Pasternak-type foundation, where the Winkler medium represented by stiffness of the springs and magnetic field parameter represents shear coefficients of the Pasternak foundation, as shown in reference [Murmu et al. 2012a].

5. Conclusions

On the basis of the Euler–Bernoulli beam theory and Eringen nonlocal elasticity, this paper investigates a compressive nonlocal double single-walled carbon nanotube (SWCNT) system, under the influence of an axial magnetic field. The dynamic responses of the DSWCNT system for four different cases of external transversal load are considered. By using the nonlocal Euler–Bernoulli beam theory and classical Maxwell relation, the system of two nonhomogeneous partial differential equations of transversal motion is derived for the coupled DNBS. Closed form solutions for natural frequencies, amplitude ratio and forced vibration response under the influence of the magnetic field and the nonlocal parameter for four cases of external excitation are obtained by applying the method of separation of variables.

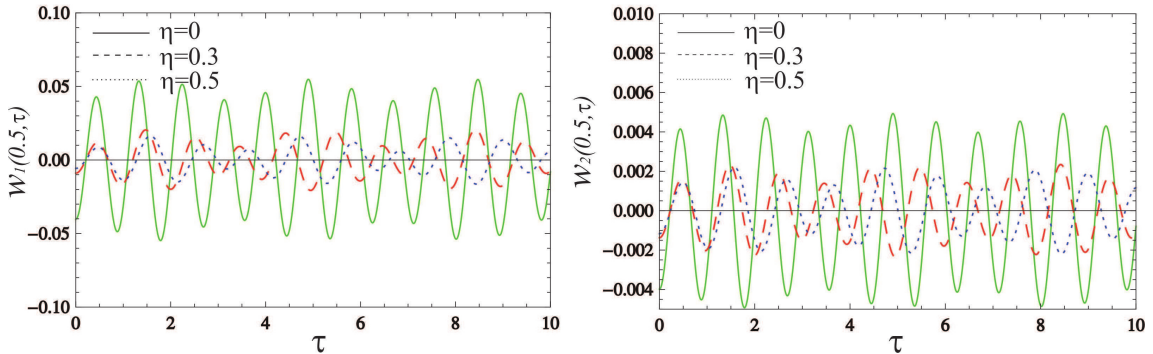


Figure 11. The relationship between forced vibrations $\bar{w}_1(0.5, \tau)$ (left) and $\bar{w}_2(0.5, \tau)$ (right) and dimensionless time for different nonlocal parameters η in the case of the moving concentrated harmonic force.

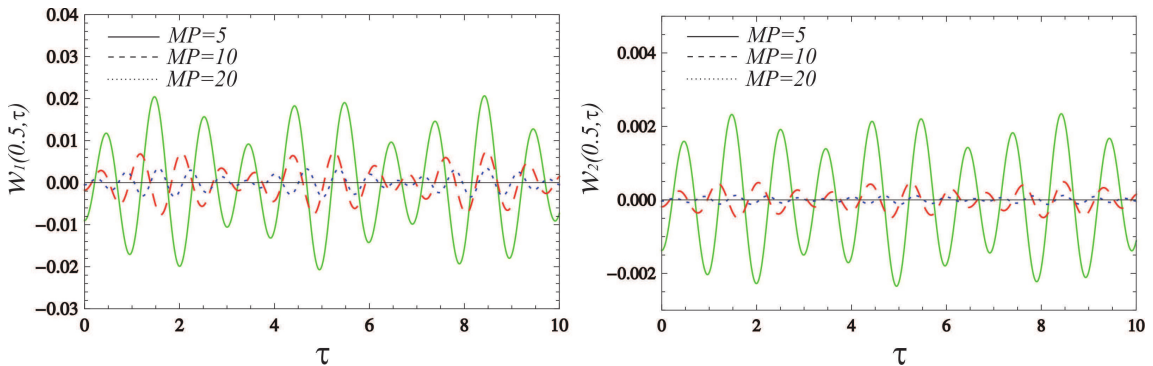


Figure 12. The relationship between forced vibrations $\bar{w}_1(0.5, \tau)$ (left) and $\bar{w}_2(0.5, \tau)$ (right) and dimensionless time for different axial magnetic fields MP in the case of the moving concentrated harmonic force.

Analytical expressions for the steady-state vibration amplitudes of the two nanobeams with the influence of the magnetic field and the nonlocal parameter are obtained, and numerical results based on them are presented. From the obtained results, we found that the nonlocal parameter and longitudinal magnetic field have a damping effect on the response vibration amplitude. In order to validate our results we compared the obtained results for the steady-state amplitude ratios with the results found in the literature and excellent agreement was achieved. It was found that the natural frequencies and response vibration amplitude of the system can change by varying the intensity of the axial magnetic field without the necessity to change any other material and geometric parameter of the DNBS. We analyzed amplitudes of transversal displacements for four cases of external excitation vibration and numerically presented the case of the uniformly distributed harmonic load and the case of the moving harmonic concentrated force with different nonlocal parameters and different axial magnetic fields. The obtained amplitudes of transversal vibration in both cases of external excitation are reduced due to the influence of the axial magnetic field. We noted that the effect of the magnetic field allows a change in the stiffness of carbon nanotubes and therefore a change in the overall stiffness of the DNBS. Changing the stiffness of the

system causes changes in the natural frequency of the system, thus avoiding the resonance region for different cases of external excitation. This possibility has great practical importance in the design of NEMS devices such as nanoactuators, nanoresonators, dynamic absorbers and nanocomposite structures based on the CNTs. Also, to validate the present analysis, MD simulations were conducted for an armchair SWCNT with different aspect ratios. The results predicted by the present model are found to be in agreement with the ones obtained from MD simulation, which indicates the capability of the present approach in accurately predicting frequencies of SWCNTs.

Acknowledgments

This research was supported by the research grant of the Serbian Ministry of Science and Environmental Protection under the number OI 174001 and OI 174011.

References

- [Adhikari and Chowdhury 2010] S. Adhikari and R. Chowdhury, “The calibration of carbon nanotube based biosensors”, *J. Appl. Phys.* **107**:12 (2010), Art. ID 124322.
- [Ajayan et al. 2006] P. M. Ajayan, L. S. Schadler, and P. V. Braun (editors), *Nanocomposite science and technology*, Wiley, Weinheim, 2006.
- [Aksencer and Aydogdu 2012] T. Aksencer and M. Aydogdu, “Forced transverse vibration of nanoplates using nonlocal elasticity”, *Physica E* **44**:7–8 (2012), 1752–1759.
- [Ansari and Sahmani 2012] R. Ansari and S. Sahmani, “Small scale effect on vibrational response of single-walled carbon nanotubes with different boundary conditions based on nonlocal beam models”, *Commun. Nonlinear Sci. Numer. Simul.* **17**:4 (2012), 1965–1979.
- [Ansari et al. 2012] R. Ansari, R. Gholami, and H. Rouhi, “Vibration analysis of single-walled carbon nanotubes using different gradient elasticity theories”, *Compos. B Eng.* **43**:8 (2012), 2985–2989.
- [Arani et al. 2013] A. H. G. Arani, M. J. Maboudi, A. G. Arani, and S. Amir, “2D-magnetic field and biaxial in-plane pre-load effects on the vibration of double bonded orthotropic graphene sheets”, *J. Solid Mech.* **5**:2 (2013), 193–205.
- [Avouris et al. 2007] P. Avouris, Z. Chen, and V. Perebeinos, “Carbon-based electronics”, *Nat. Nanotechnol.* **2**:10 (2007), 605–615.
- [Barone and Peralta 2008] V. Barone and J. E. Peralta, “Magnetic boron nitride nanoribbons with tunable electronic properties”, *Nano Lett.* **8**:8 (2008), 2210–2214.
- [Bellucci et al. 2007] S. Bellucci, J. González, F. Guinea, P. Onorato, and E. Perfetto, “Magnetic field effects in carbon nanotubes”, *J. Phys. Condens. Matter* **19**:39 (2007), 395017.
- [Claeyssen et al. 2013] J. R. Claeysen, T. Tsukazan, and R. D. Coppeti, “Nonlocal effects in modal analysis of forced responses with single carbon nanotubes”, *Mech. Syst. Signal Process.* **38**:2 (2013), 299–311.
- [Correa-Duarte et al. 2005] M. A. Correa-Duarte, M. Grzelczak, V. Salgueiriño-Maceira, M. Giersig, L. M. Liz-Marzán, M. Farle, K. Sieradzki, and R. Diaz, “Alignment of carbon nanotubes under low magnetic fields through attachment of magnetic nanoparticles”, *J. Phys. Chem. B* **109**:41 (2005), 19060–19063.
- [Şimşek 2010a] M. Şimşek, “Dynamic analysis of an embedded microbeam carrying a moving microparticle based on the modified couple stress theory”, *Int. J. Eng. Sci.* **48**:12 (2010), 1721–1732.
- [Şimşek 2010b] M. Şimşek, “Vibration analysis of a single-walled carbon nanotube under action of a moving harmonic load based on nonlocal elasticity theory”, *Physica E* **43**:1 (2010), 182–191.
- [Şimşek 2011] M. Şimşek, “Nonlocal effects in the forced vibration of an elastically connected double-carbon nanotube system under a moving nanoparticle”, *Comput. Mater. Sci.* **50**:7 (2011), 2112–2123.

- [Dresselhaus et al. 2005] M. S. Dresselhaus, G. Dresselhaus, R. Saito, and A. Jorio, "Raman spectroscopy of carbon nanotubes", *Phys. Rep.* **409**:2 (2005), 47–99.
- [Duan et al. 2007] W. H. Duan, C. M. Wang, and Y. Y. Zhang, "Calibration of nonlocal scaling effect parameter for free vibration of carbon nanotubes by molecular dynamics", *J. Appl. Phys.* **101**:2 (2007), Art. ID 024305.
- [Dubay and Kresse 2003] O. Dubay and G. Kresse, "Accurate density functional calculations for the phonon dispersion relations of graphite layer and carbon nanotubes", *Phys. Rev. B* **67**:3 (2003), 035401.
- [Eringen 1972] A. C. Eringen, "Linear theory of nonlocal elasticity and dispersion of plane waves", *Int. J. Eng. Sci.* **10**:5 (1972), 425–435.
- [Eringen 1983] A. C. Eringen, "On differential equations of nonlocal elasticity and solutions of screw dislocation and surface waves", *J. Appl. Phys.* **54**:9 (1983), 4703–4710.
- [Eringen 2002] A. C. Eringen, *Nonlocal continuum field theories*, Springer, New York, 2002.
- [Eringen and Edelen 1972] A. C. Eringen and D. G. B. Edelen, "On nonlocal elasticity", *Int. J. Eng. Sci.* **10**:3 (1972), 233–248.
- [Ghorbanpour Arani and Shokravi 2014] A. Ghorbanpour Arani and M. Shokravi, "Vibration response of visco-elastically coupled double-layered visco-elastic graphene sheet systems subjected to magnetic field via strain gradient theory considering surface stress effects", *Proc. Inst. Mech. Eng. N J. Nanoeng. Nanosyst.* (online publication April 2014).
- [Goerbig et al. 2006] M. O. Goerbig, R. Moessner, and B. Douçot, "Electron interactions in graphene in a strong magnetic field", *Phys. Rev. B* **74**:16 (2006), 161407.
- [Hata et al. 2004] K. Hata, D. N. Futaba, K. Mizuno, T. Namai, M. Yumura, and S. Iijima, "Water-assisted highly efficient synthesis of impurity-free single-walled carbon nanotubes", *Science* **306**:5700 (2004), 1362–1364.
- [Hu et al. 1999] J. Hu, T. W. Odom, and C. M. Lieber, "Chemistry and physics in one dimension: Synthesis and properties of nanowires and nanotubes", *Acc. Chem. Res.* **32**:5 (1999), 435–445.
- [Iijima 1991] S. Iijima, "Helical microtubules of graphitic carbon", *Nature* **354**:6348 (1991), 56–58.
- [Iijima et al. 1996] S. Iijima, C. Brabec, A. Maiti, and J. Bernholc, "Structural flexibility of carbon nanotubes", *J. Chem. Phys.* **104**:5 (1996), 2089–2092.
- [Kacem et al. 2011] N. Kacem, S. Baguet, S. Hentz, and R. Dufour, "Computational and quasi-analytical models for non-linear vibrations of resonant MEMS and NEMS sensors", *Int. J. Non-Linear Mech.* **46**:3 (2011), 532–542.
- [Karličić et al. 2014a] D. Karličić, S. Adhikari, T. Murmu, and M. Cajić, "Exact closed-form solution for non-local vibration and biaxial buckling of bonded multi-nanoplate system", *Compos. B Eng.* **66** (2014), 328–339.
- [Karličić et al. 2014b] D. Karličić, P. Kozić, and R. Pavlović, "Free transverse vibration of nonlocal viscoelastic orthotropic multi-nanoplate system (MNPS) embedded in a viscoelastic medium", *Compos. Struct.* **115** (2014), 89–99.
- [Karličić et al. 2014c] D. Karličić, T. Murmu, M. Cajić, P. Kozić, and S. Adhikari, "Dynamics of multiple viscoelastic carbon nanotube based nanocomposites with axial magnetic field", *J. Appl. Phys.* **115**:23 (2014), Art. ID 234303.
- [Ke et al. 2009] L. L. Ke, Y. Xiang, J. Yang, and S. Kitipornchai, "Nonlinear free vibration of embedded double-walled carbon nanotubes based on nonlocal Timoshenko beam theory", *Comput. Mater. Sci.* **47**:2 (2009), 409–417.
- [Kiani 2012] K. Kiani, "Transverse wave propagation in elastically confined single-walled carbon nanotubes subjected to longitudinal magnetic fields using nonlocal elasticity models", *Physica E* **45** (2012), 86–96.
- [Kiani and Mehri 2010] K. Kiani and B. Mehri, "Assessment of nanotube structures under a moving nanoparticle using nonlocal beam theories", *J. Sound Vib.* **329**:11 (2010), 2241–2264.
- [Kozic et al. 2014] P. Kozic, R. Pavlović, and D. Karličić, "The flexural vibration and buckling of the elastically connected parallel-beams with a Kerr-type layer in between", *Mech. Res. Commun.* **56** (2014), 83–89.
- [Kraus 1984] J. Kraus, *Electromagnetics*, McGraw-Hill, New York, 1984.
- [Krstić et al. 2004] V. Krstić, G. Wagnière, and G. L. J. A. Rikken, "Magneto-dynamics of chiral carbon nanotubes", *Chem. Phys. Lett.* **390**:1–3 (2004), 25–28.
- [Kumar and Mohammad 2011] C. S. S. R. Kumar and F. Mohammad, "Magnetic nanomaterials for hyperthermia-based therapy and controlled drug delivery", *Adv. Drug Deliv. Rev.* **63**:9 (2011), 789–808.

- [Lazarus et al. 2012] A. Lazarus, O. Thomas, and J.-F. Deü, “Finite element reduced order models for nonlinear vibrations of piezoelectric layered beams with applications to NEMS”, *Finite Elem. Anal. Des.* **49**:1 (2012), 35–51.
- [Li and Chou 2004] C. Li and T.-W. Chou, “Mass detection using carbon nanotube-based nanomechanical resonators”, *Appl. Phys. Lett.* **84**:25 (2004), 5246–5248.
- [Li et al. 2008] C. Li, E. T. Thostenson, and T.-W. Chou, “Sensors and actuators based on carbon nanotubes and their composites: A review”, *Compos. Sci. Technol.* **68**:6 (2008), 1227–1249.
- [Liu et al. 2003] Y. Liu, R. O. Jones, X. Zhao, and Y. Ando, “Carbon species confined inside carbon nanotubes: A density functional study”, *Phys. Rev. B* **68**:12 (2003), 125413.
- [Lu 1997] J. P. Lu, “Elastic properties of carbon nanotubes and nanoropes”, *Phys. Rev. Lett.* **79**:7 (1997), 1297–1300.
- [Moniruzzaman and Winey 2006] M. Moniruzzaman and K. I. Winey, “Polymer nanocomposites containing carbon nanotubes”, *Macromolecules* **39**:16 (2006), 5194–5205.
- [Murmu and Adhikari 2011] T. Murmu and S. Adhikari, “Nonlocal vibration of carbon nanotubes with attached buckyballs at tip”, *Mech. Res. Commun.* **38**:1 (2011), 62–67.
- [Murmu and Adhikari 2012] T. Murmu and S. Adhikari, “Nonlocal frequency analysis of nanoscale biosensors”, *Sens. Actuators A Phys.* **173**:1 (2012), 41–48.
- [Murmu et al. 2012a] T. Murmu, M. A. McCarthy, and S. Adhikari, “Nonlocal elasticity based magnetic field affected vibration response of double single-walled carbon nanotube systems”, *J. Appl. Phys.* **111**:11 (2012), Art. ID 113511.
- [Murmu et al. 2012b] T. Murmu, M. A. McCarthy, and S. Adhikari, “Vibration response of double-walled carbon nanotubes subjected to an externally applied longitudinal magnetic field: A nonlocal elasticity approach”, *J. Sound Vib.* **331**:23 (2012), 5069–5086.
- [Narendar et al. 2012] S. Narendar, S. S. Gupta, and S. Gopalakrishnan, “Wave propagation in single-walled carbon nanotube under longitudinal magnetic field using nonlocal Euler–Bernoulli beam theory”, *Appl. Math. Model.* **36**:9 (2012), 4529–4538.
- [Oniszczuk 2003] Z. Oniszczuk, “Forced transverse vibrations of an elastically connected complex simply supported double-beam system”, *J. Sound Vib.* **264**:2 (2003), 273–286.
- [Popov et al. 2014] A. M. Popov, I. V. Lebedeva, A. A. Knizhnik, Y. E. Lozovik, N. A. Poklonski, A. I. Siahlo, S. A. Vyrko, and S. V. Ratkevich, “Force and magnetic field sensor based on measurement of tunneling conductance between ends of coaxial carbon nanotubes”, *Comput. Mater. Sci.* **92** (2014), 84–91.
- [Reich et al. 2008] S. Reich, C. Thomsen, and J. Maultzsch, *Carbon nanotubes: Basic concepts and physical properties*, Wiley, Weinheim, 2008.
- [Roth and Baughman 2002] S. Roth and R. H. Baughman, “Actuators of individual carbon nanotubes”, *Curr. Appl. Phys.* **2**:4 (2002), 311–314.
- [Ru 2001] C. Q. Ru, “Axially compressed buckling of a doublewalled carbon nanotube embedded in an elastic medium”, *J. Mech. Phys. Solids* **49**:6 (2001), 1265–1279.
- [Ruoff et al. 2003] R. S. Ruoff, D. Qian, and W. K. Liu, “Mechanical properties of carbon nanotubes: Theoretical predictions and experimental measurements”, *C. R. Phys.* **4**:9 (2003), 993–1008.
- [Saito 2003] Y. Saito, “Carbon nanotube field emitter”, *J. Nanosci. Nanotechnol.* **3**:1–2 (2003), 39–50.
- [Salvetat et al. 1999] J.-P. Salvetat, J.-M. Bonard, N. H. Thomson, A. J. Kulik, L. Forró, W. Benoit, and L. Zuppiroli, “Mechanical properties of carbon nanotubes”, *Appl. Phys. A Mater. Sci. Process.* **69**:3 (1999), 255–260.
- [Slavcheva and Roussignol 2011] G. Slavcheva and P. Roussignol, “Coherent magneto-optical polarisation dynamics in a single chiral carbon nanotube”, *Superlattices Microstruct.* **49**:3 (2011), 325–330.
- [Yang et al. 2010] J. Yang, L. L. Ke, and S. Kitipornchai, “Nonlinear free vibration of single-walled carbon nanotubes using nonlocal Timoshenko beam theory”, *Physica E* **42**:5 (2010), 1727–1735.
- [Zhang et al. 2008] Y. Q. Zhang, Y. Lu, and G. W. Ma, “Effect of compressive axial load on forced transverse vibrations of a double-beam system”, *Int. J. Mech. Sci.* **50**:2 (2008), 299–305.

Received 25 May 2015. Revised 30 Sep 2015. Accepted 1 Jan 2016.

MARIJA B. STAMENKOVIĆ: s_marija86@yahoo.com

Mathematical Institute of the Serbian Academy of Science and Arts, Kneza Mihaila 36, 11001 Belgrade, Serbia

DANILO KARLIČIĆ: danilo.karlicic@masfak.ni.ac.rs

Faculty of Mechanical Engineering, University of Niš, A. Medvedeva 14, 18000 Niš, Serbia

GORAN JANEVSKI: gocky.jane@gmail.com

Department of Mechanical Engineering, University of Niš, A. Medvedeva 14, 18000 Niš, Serbia

PREDRAG KOZIĆ: kozicp@yahoo.com

Faculty of Mechanical Engineering, University of Niš, A. Medvedeva 14, 18000 Niš, Serbia

JOURNAL OF MECHANICS OF MATERIALS AND STRUCTURES

msp.org/jomms

Founded by Charles R. Steele and Marie-Louise Steele

EDITORIAL BOARD

ADAIR R. AGUIAR	University of São Paulo at São Carlos, Brazil
KATIA BERTOLDI	Harvard University, USA
DAVIDE BIGONI	University of Trento, Italy
YIBIN FU	Keele University, UK
IWONA JASIUK	University of Illinois at Urbana-Champaign, USA
C. W. LIM	City University of Hong Kong
THOMAS J. PENCE	Michigan State University, USA
GIANNI ROYER-CARFAGNI	Università degli studi di Parma, Italy
DAVID STEIGMANN	University of California at Berkeley, USA
PAUL STEINMANN	Friedrich-Alexander-Universität Erlangen-Nürnberg, Germany

ADVISORY BOARD

J. P. CARTER	University of Sydney, Australia
D. H. HODGES	Georgia Institute of Technology, USA
J. HUTCHINSON	Harvard University, USA
D. PAMPLONA	Universidade Católica do Rio de Janeiro, Brazil
M. B. RUBIN	Technion, Haifa, Israel

PRODUCTION production@msp.org

SILVIO LEVY Scientific Editor

See msp.org/jomms for submission guidelines.

JoMMS (ISSN 1559-3959) at Mathematical Sciences Publishers, 798 Evans Hall #6840, c/o University of California, Berkeley, CA 94720-3840, is published in 10 issues a year. The subscription price for 2016 is US\$575/year for the electronic version, and \$735/year (+\$60, if shipping outside the US) for print and electronic. Subscriptions, requests for back issues, and changes of address should be sent to MSP.

JoMMS peer-review and production is managed by EditFLOW[®] from Mathematical Sciences Publishers.

PUBLISHED BY

 **mathematical sciences publishers**
nonprofit scientific publishing

<http://msp.org/>

© 2016 Mathematical Sciences Publishers

Journal of Mechanics of Materials and Structures

Volume 11, No. 3

May 2016

- An Eulerian formulation for large deformations of elastically isotropic elastic-viscoplastic membranes** M. B. RUBIN and BEN NADLER 197
- Physical meaning of elastic constants in Cosserat, void, and microstretch elasticity** RODERIC S. LAKES 217
- On low-frequency vibrations of a composite string with contrast properties for energy scavenging fabric devices** ASKAR KUDAIBERGENOV, ANDREA NOBILI and LUDMILLA PRIKAZCHIKOVA 231
- Wave propagation in layered piezoelectric rings with rectangular cross sections** JIANGONG YU, XIAODONG YANG and JEAN-ETIENNE LEFEBVRE 245
- Effective boundary condition method and approximate secular equations of Rayleigh waves in orthotropic half-spaces coated by a thin layer** PHAM CHI VINH and VU THI NGOC ANH 259
- Nonlocal forced vibration of a double single-walled carbon nanotube system under the influence of an axial magnetic field** MARIJA B. STAMENKOVIĆ, DANILO KARLIČIĆ, GORAN JANEVSKI and PREDRAG KOZIĆ 279
- A phase-field model of quasistatic and dynamic brittle fracture using a staggered algorithm** HAMDİ HENTATI, MARWA DHAHRI and FAKHREDDINE DAMMAK 309



1559-3959(2016)11:3;1-6